emIAM v1.0: an emulator for Integrated Assessment Models using marginal abatement cost curves

Weiwei Xiong[1,2], Katsumasa Tanaka[1,3], Philippe Ciais[1], Daniel J. A. Johansson[4], Mariliis Lehtveer[4]

[1] Laboratoire des Sciences du Climat et de l'Environnement (LSCE), IPSL, CEA/CNRS/UVSQ, Université Paris-Saclay, Gif-sur-Yvette, 91191, France

[2] School of Economics and Management, China University of Geosciences, Wuhan, 430074, China

[3] Earth System Division, National Institute for Environmental Studies (NIES), Tsukuba, 305-8506, Japan

[4] Division of Physical Resource Theory, Department of Space, Earth, and Environment, Chalmers University of Technology, Gothenburg, 412 96, Sweden

Correspondence to: Weiwei Xiong (weiwei.xiong@lsce.ipsl.fr) and Katsumasa Tanaka (katsumasa.tanaka@lsce.ipsl.fr)

Abstract. We developed an emulator for Integrated Assessment Models (emIAM) based on a marginal abatement cost (MAC) curve approach. Drawing on the output of IAMs in the ENGAGE Scenario Explorer and the GET model, we derived an extensive array of MAC curves, encompassing ten IAMs, global and ten regions, three gases CO_2, CH_4, and N_2O, eight portfolios of available mitigation technologies, and two emission sources. We tested the performance of emIAM by coupling it with a simple climate model ACC2. Our analysis showed that the optimizing climate-economy model ACC2-emIAM adequately reproduced a majority of the original IAM emission outcomes under similar conditions. This can facilitate systematic exploration of IAMs with small computational resources. emIAM holds the potential to enhance the capabilities of simple climate models as a tool for calculating cost-effective pathways directly aligned with temperature targets.

1 Introduction

Integrated Assessment Models (IAMs) combine economic, energy, and sometimes also land-use modeling approaches and are commonly used to evaluate least-cost mitigation scenarios (Weyant, 2017). A variety of IAMs were integrated under common protocols in modeling intercomparison projects (MIPs) (O'Neill et al., 2016; Tebaldi et al., 2021) and provided input to the series of the Intergovernmental Panel on Climate Change (IPCC) Assessment Reports. However, simulating computationally expensive IAMs developed and maintained at different research institutions around the world requires large coordination efforts. Therefore, here we propose a new methodological framework to i) emulate the behavior of IAMs (i.e., emission abatement for a given carbon price) through MAC curves and then ii) reproduce the behavior of IAMs by using the MAC curves coupled with a simple climate model. We show that the MAC curves can be systematically applied to reproduce the behavior of IAMs as an emulator for IAMs (emIAM), paving a way to generate multi-IAM scenarios more easily than before, with small computational resources.

In the context of climate change mitigation, a MAC generally represents the incremental cost of reducing an additional

Deleted: Tanaka[2]
Deleted: Ciais[2]
Deleted: [1] School of Economics and Management, China University of Geosciences, Wuhan, 430074, China [2]
Deleted: xww08012115@cug.edu.cn
Deleted: Using
Deleted: a large set
Deleted: :
Deleted: ;
Deleted: eleven
Deleted: ;
Deleted: ;
Deleted: ;
Deleted: We found
Deleted: -ACC2
Deleted: , allowing
Deleted: explorations
Deleted: can expand the capability
Deleted: to calculate
Deleted: linked
Deleted: to a
Deleted: target
Deleted: economy
Deleted: climate policies under
Deleted: A variety of IAMs were integrated under common protocols in modeling intercomparison projects (MIPs) (O'Neill et al., 2016)
Deleted: Simulating
Deleted: institutes
Deleted: , however,
Deleted: (Ellerman and Decaux, 1998; Klepper and Peterson, 2006)Here
Deleted: emerging
Deleted: marginal abatement cost (
Deleted:)

unit of emissions; a MAC curve illustrates these costs as the level of emission reductions increases relative to the baseline. There is a burgeoning literature on MAC curves (Jiang et al., 2020) that can broadly fall into two categories (Kesicki and Ekins, 2012): i) data-based MAC curves (bottom-up) and ii) model-based MAC curves (top-down). First, a data-based MAC curve provides a relationship between the emission abatement potential of each mitigation measure considered and the associated marginal costs, in the order of low- to high-cost measures based on individual data. A prominent example of such data-based MAC curves is McKinsey & Company (2009). Second, a model-based MAC curve provides a relationship between the amount of emission abatement and the system-wide marginal costs based on simulation results of a model (e.g., an energy system model and a computational general equilibrium (CGE) model) perturbed under different carbon prices or carbon budgets. Our work takes the second approach, building on previous studies (Nordhaus, 1991; Ellerman and Decaux, 1998; Vuuren et al., 2004; Johansson et al., 2006; Klepper and Peterson, 2006; Johansson, 2011; Morris et al., 2012; Wagner et al., 2012; Tanaka et al., 2013; Su et al., 2017; Tanaka and O'Neill, 2018; Yue et al., 2020; Tanaka et al., 2021). While data-based MAC curves tend to be rich in the representation of technological details, they do not consider system-wide interactions that are captured by model-based MAC curves. Model-based MAC curves reflect such interactions, however, without much explicit technological detail. Advantages and disadvantages of MAC curves of different categories are discussed elsewhere (Vermont and De Cara, 2010; Kesicki and Strachan, 2011; Huang et al., 2016).

In this study, we derive a large set of MAC curves from the simulation results of IAMs (see Figure 1 and Section 3), couple them with a simple climate model as an emulator (emIAM), and validate the simulation results with the original IAM results under similar conditions. Namely, we look up the ENGAGE Scenario Explorer hosted at IIASA, Austria (https://data.ene.iiasa.ac.at/engage), a publicly available database from the EU Horizon 2020 ENGAGE project (Riahi et al., 2021; Drouet et al., 2021), and extract total anthropogenic CO_2, CH_4, and N_2O emission pathways until 2100 from nine IAMs under a range of carbon budget constraints. For each IAM, we derive a set of CO_2, CH_4, and N_2O MAC curves as a function of the respective emission reduction in percentage relative to the baseline at the global and regional (ten regions) levels. We then integrate the sets of MAC curves (i.e., emIAM) into a simple climate model called the Aggregated Carbon Cycle, Atmospheric Chemistry, and Climate (ACC2) model (Tanaka et al., 2007; Tanaka and O'Neill, 2018; Xiong et al., 2022). ACC2-emIAM works as a hard-linked optimizing climate-economy model that can derive an emission pathway to achieve a given climate target or carbon budget at the lowest cost. We validate to what extent the emission pathway derived from ACC2-emIAM under a given carbon budget or a temperature target can reproduce the corresponding pathway from the original IAM in the ENGAGE Scenario Explorer.

We further apply the emIAM approach to the GET model (Lehtveer et al., 2019), an IAM that did not take part in the ENGAGE project. We can directly simulate GET to derive MAC curves under different model configurations, which complements the existing data from IAMs simulated under single configurations for the ENGAGE project. We obtain global energy-related CO_2 emission pathways under a range of carbon price projections, but with several different portfolios of

Deleted: gives
Deleted: from
Deleted: of the
Deleted: measures
Deleted: gives
Deleted: earlier
Deleted: This
Deleted: derives
Deleted: , couples
Deleted: as an emulator (emIAM)
Deleted: ,
Deleted: validates
Deleted: levels (eleven
Deleted:).
Deleted: implement
Deleted: -ACC2
Deleted: where total cost of mitigation is optimized under a…
Deleted: .
Deleted: -ACC2
Deleted: certain
Deleted: : we

available mitigation technologies (e.g., differentiated Carbon Capture and Storage (CCS) capacity). We then derive a MAC curve for each technology portfolio. Although MAC curves concern only the total emission abatement without distinguishing individual mitigation measures, this approach allows us to explore the role of a particular mitigation measure by comparing MAC curves with and without that mitigation measure. Note that all IAMs emulated in this study take a cost-effectiveness approach, in which the least-cost emission pathways to achieve a climate-related target are calculated in terms of the cost of mitigation without considering climate damage and adaptation.

To our knowledge, this study is one of the first attempts to apply the MAC curve approach extensively for developing an IAM emulator: we consider ten IAMs, global and ten regions, three gases (i.e., CO_2, CH_4, and N_2O), eight technology portfolios, and two broad sources (i.e., total anthropogenic and energy-related emissions). We demonstrate the applicability of emIAM by implementing it to ACC2, but emIAM can also be used with other simple climate models (Joos et al., 2013; Nicholls et al., 2020). Thus, emIAM allows ACC2 and potentially other simple climate models to reproduce approximately global and regional cost-effective emission pathways from multiple IAMs under a range of given carbon budgets or temperature targets. In recent years, there have been efforts to develop emulators of Earth System Models (ESMs) in CMIP6 and the use of ESM emulators was exploited in the IPCC Sixth Assessment Report (AR6) (Leach et al., 2021; Tsutsui, 2022); however, no emulator has yet been developed for IAMs contributing to the IPCC.

In this paper, following the common definitions of terminologies found in the literature (National Research Council, 2012; Mulugeta et al., 2018), we use "emulate" to indicate a process of identifying a reduced-complexity model (i.e., a MAC curve) that approximates the behavior of a complex model (i.e., an IAM), "reproduce" to refer to a process of generating an output (i.e., an emission pathway) from an emulator with the same input and constraints given to an IAM (i.e., a cumulative carbon budget or end-of-century temperature, for example), and "validate" to indicate a process of investigating the extent to which an emulator reproduces an intended outcome in comparison to the corresponding original outcome from an IAM. Regarding the units, we use the original units of each model (i.e., US$2010 and tCO_2-eq with 100-year Global Warming Potential (GWP100) for all IAMs emulated here) to keep the comparability with underlying data, unless noted otherwise.

The remainder of the manuscript consists of four sections: Section 2 introduces the IAMs under consideration and their experiments used to derive MAC curves. Section 3 describes the methodology to derive MAC curves and presents the MAC curves that are derived (i.e., emIAM). Section 4 shows the validation results for ACC2-emIAM. The paper is concluded in Section 5 with general remarks on the utility of emIAM. Given the substantial amount of MAC curves generated in our analysis, results are presented only selectively in the main body of the paper; a more extensive and systematic presentation of the results can be found in Supplement and our Zenodo repository.

2 IAMs to emulate

Our study uses the output from a total of ten IAMs: nine IAMs used in the ENGAGE project and another IAM GET. The

Deleted: each

Deleted: curve concerns

Deleted: specific

Deleted: the outcomes based on

Deleted: this

Deleted: eleven

Deleted: also

Deleted: and

Deleted: efforts

Deleted: made

Deleted: latest

Deleted: .

Moved down [1]: Section 3 describes the methodology to derive MAC curves and presents the MAC curves that are derived (i.e., emIAM).

Deleted: The rest of the manuscript consists of four sections: Section 2 introduces the IAMs and the experiments used to derive MAC curves.

Deleted: Section 4 shows the validation results for emIAM-ACC2. The paper is concluded with general remarks on the use of emIAM in Section 5. Due to the large number of MAC curves spanning several dimensions, there are a vast amount of display items from our analysis. Results are only selectively shown in the main paper; they are more comprehensively and systematically presented in the Supplement and our Zenodo repository.
Following

Deleted: (National Research Council, 2012; Mulugeta et al., 2018)…

Deleted: the-

Deleted: tCO_2

Moved (insertion) [1]

Deleted: **2 IAMs to emulate**
Our study uses the output from a total of ten IAMs: nine IAMs used in the ENGAGE project and another IAM GET. (Riahi et al., 2022)The subsections below describe these IAMs and their data used to derive MAC curves.

subsections below describe these IAMs and their data used to derive MAC curves.

2.1 IAMs from the ENGAGE project

We selected the following nine IAM versions available in the database of the ENGAGE Scenario Explorer: AIM/CGE V2.2, COFFEE 1.1, GEM-E3 V2021, IMAGE 3.0, MESSAGEix-GLOBIOM 1.1, POLES-JRC ENGAGE, REMIND-MAgPIE 2.1-4.2, TIAM-ECN 1.1, and WITCH 5.0 (thereafter, shorter labels indicated in Table 1 will be used). These IAMs are diverse in terms of solution concepts (general equilibrium and partial equilibrium models) and solution methods (intertemporal optimization and recursive dynamic models) (Table 1), among many other perspectives (Guivarch et al., 2022). A series of scenarios following a carbon budget ranging from 200 to 3,000 $GtCO_2$ (for the period of 2019-2100), as well as baseline scenarios, are available from each IAM. All scenarios incorporate second marker baseline scenario from the Shared Socioeconomic Pathways (SSP2), which reflect middle-of-the-road socioeconomic conditions (Riahi et al., 2017). The ENGAGE Scenario Explorer is now part of the larger IPCC Sixth Assessment Report (AR6) Scenario Explorer (Byers et al., 2022), which was not available at the time of our analysis. Although the use of the entire AR6 scenario dataset could be advantageous in terms of the number of IAMs and scenarios available for analyses (189 IAMs (including different model versions) and 1389 scenarios in the AR6 Scenario Explorer; 20 IAMs (including different model versions) and 231 scenarios in the ENGAGE Scenario Explorer), an advantage of using the ENGAGE Scenario Explorer is that the data from IAMs were obtained under a common experimental protocol, allowing consistent analyses.

There are two types of scenarios in the ENGAGE Scenario Explorer: i) end-of-century budget (ECB) scenarios (with "f" in the original scenario name) and ii) peak budget (PKB) scenarios (without "f" in the original scenario name) (Riahi et al., 2021). While the former type of scenarios is defined with a carbon budget till the end of this century, including a possibility of temporarily overspending it before (i.e., a possibility of achieving net negative CO_2 emissions), the latter type of scenarios is defined with a carbon budget without allowing temporal budget overspending (i.e., a possibility of achieving net-zero CO_2 emissions, but not net negative CO_2 emissions). The distinction of the two sets of scenarios may have important near-term implications (Johansson, 2021) and are considered when MAC curves are derived. For each type of scenarios, there are another two types of scenarios: i) scenarios without INDC, which only consider currently implemented national policies (indicated as "NPi2020" in the original scenario name); ii) scenarios with INDC, which further consider national emission pledges until 2030 (indicated as "INDCi2030" in the original scenario name). The availability of scenarios depends on the types of scenarios and varies across IAMs. For each IAM, we used the NPi2100 scenario, a scenario assuming a continuation of current stated policies until 2100, as the baseline scenario for all carbon budget scenarios in our analysis. The NPi2100 scenarios, which are available for all IAMs considered here, are only slightly different from the NoPolicy scenarios assuming no climate policies at all.

The ENGAGE Scenario Explorer contains emission data for many greenhouse gases (GHGs) and air pollutants from each IAM, including CO_2, CH_4, and N_2O emissions analyzed in our study. Emission data are available at global and regional

Deleted: Nine IAMs are

Deleted: as in Table 1

Deleted: net-negative emissions

Deleted: implying a temperature overshoot;

Deleted: net-zero CO_2 emissions

Deleted: implying a limited or no temperature overshoot;

Deleted: till the point of meeting net-zero CO_2 emissions

Deleted: a

Deleted: .

Deleted: NPi2020

Deleted: ;

Deleted: INDCi2030

Deleted: .

Deleted: We

levels (for nine and five IAMs, respectively). There are two sets of regional emission data, with one for five regions and the other for ten regions, the latter of which was used in our study: that is, China (CHN), European Union and Western Europe (EUWE), Latin America (LATAME), Middle East (MIDEAST), North America (NORAM), Other Asian countries (OTASIAN), Pacific OECD (PACOECD), Reforming Economies (REFECO), South Asia (SOUASIA), and Sub-Saharan Africa (SUBSAFR). Although all ENGAGE IAMs are regionally disaggregated, only a subset of the IAMs provides data for ten regions in the ENGAGE Scenario Explore as shown in Table 1. Note that the GEM model provides emissions for Rest of World (ROW), one more region in addition to the ten regions, in the ENGAGE Scenario Explorer. In other IAMs, we also allocated emissions for ROW to account for the discrepancy between global emissions and the sum of regional emissions (e.g., 3% difference in CO_2 emissions in AIM/CGE V2.2). Regarding emission sources, total anthropogenic emissions and energy-related emissions (e.g., energy and industrial processes) were separately used to derive global MAC curves for three gases (only total anthropogenic emissions for regional MAC curves due to computational requirements for validating regional MAC curves). Non-energy-related emissions (e.g., agriculture, forestry, and land-use sector), the differences between the two, were not used to generate MAC curves because non-energy-related emissions did not appear to be strongly correlated with carbon prices in most IAMs in the ENGAGE project.

Deleted:), and Rest of World (ROW

Deleted: only

Deleted: for generating

Deleted: and influenced by other factors (Oliveira et al., 2021).

2.2 GET model

GET is a global energy system model designed to study climate mitigation and energy strategies to achieve long-term climate targets under exogenously given energy demand scenarios (Azar et al., 2003; Hedenus et al., 2010; Azar et al., 2013; Lehtveer and Hedenus, 2015; Lehtveer et al., 2019). It is an intertemporal optimization model that, with perfect foresight, minimizes the total cost of the energy system discounted over the simulation period till 2150 (default discount rate of 5%). To do so, various technologies for converting and supplying energy are evaluated in the model. The model considers primary energy sources such as coal, natural gas, oil, biomass, solar, nuclear, wind, and hydropower. Energy carriers considered in the model are petroleum fuels (gasoline, diesel, and natural gas), synthetic fuels (e.g., methanol), hydrogen, and electricity. End-use sectors in the model are transport, feedstock, residential heat, industrial heat, and electricity. We employed GET version 10.0 (Lehtveer et al., 2019) with the representation of ten regions.

Deleted: minimizes

Deleted: costs

Deleted: 5%

Deleted: by default).

To develop global energy-related CO_2 MAC curves reflecting different sets of available mitigation measures, we constructed the following eight technology portfolios: i) Base, ii) Optimistic, iii) Pessimistic, iv) No CCS+Carbon Capture and Utilization (CCU)+Direct Air Capture (DAC), v) Large bioenergy, vi) Large bioenergy + Small carbon storage, vii) Small bioenergy + Large carbon storage, and viii) No nuclear. The Base portfolio uses the default set of assumptions associated with mitigation options available in the model. The Optimistic portfolio combines the assumptions of Large bioenergy supply, Large carbon storage potential, CCS+CCU+DAC, and Nuclear power. The Pessimistic portfolio, in contrast, combines those of Small bioenergy supply, Small carbon storage potential, No CCS+CCU+DAC, and No nuclear power. Large and Small bioenergy cases assume 100% more and 50% less bioenergy, respectively, than the default level (134 EJ/year globally). Large

Deleted: set up

Deleted: on the contrary

Deleted: larger

Deleted: smaller

Deleted: levels

and Small carbon storage cases assume 8,000 $GtCO_2$ and 1,000 $GtCO_2$, respectively (2,000 $GtCO_2$ by default). With each of these technology portfolios, we simulated the model under 22 different carbon price scenarios. In all carbon price scenarios, the carbon price grows 5% each year with a range of initial levels in 2010 (1, 2, 3, 5, 7, 10, …, 140 US$2010/$tCO_2$) (see Table S1 for details), following the principle of the Hotelling rule where there is a limit on the cumulative emissions (Hof et al., 2021). We assumed a discount rate of 5% for all portfolios and carbon price scenarios. Our analysis used a scenario with zero carbon prices as the baseline scenario. We derived only global energy-related CO_2 MAC curves from GET since the model does not explicitly describe processes related to non-energy related emissions.

3 Development of emIAM

3.1 Deriving MAC curves

Our MAC curve approach aims to capture the relationship between the carbon price and the emission abatement in IAMs. For each IAM (i.e., ENGAGE IAMs and GET), we calculated the emission reduction level relative to the respective baseline level at each time step. Emission reductions can be expressed either in absolute terms (for example, in $GtCO_2$) or in percentage terms (in percentage relative to the baseline level) (Kesicki, 2013; Jiang et al., 2022), the latter of which is used in our analysis. When the emission is at the baseline level, the relative emission reduction is, by definition, 0%. When it is 100%, which can occur for CO_2, the emission is (net) zero. When it exceeds 100%, the emission becomes (net) negative. The carbon price for each case is also the relative level to the baseline scenario. If there are non-zero carbon prices in the baseline scenarios (small carbon prices can be found in baseline scenarios from some IAMs), we subtracted them from the carbon prices in the mitigation scenarios. The MAC curves were derived from the data for the period 2020-2100 in the case of ENGAGE IAMs and GET (we did not consider the data from GET after 2100).

There are three key assumptions in our approach: i) MAC curves are assumed to be time-independent, ii) abatement levels are assumed to be independent across gases, and iii) abatement levels are assumed to be independent across regions. While MAC curves are more commonly time-dependent or for a specific point in time, time-independent MAC curves have also been used for long-term pathway calculations (Johansson et al., 2006; Tanaka and O'Neill, 2018; Tanaka et al., 2021) and short-term assessments (De Cara and Jayet, 2011). The implications of the first assumption are discussed later in this section. The second assumption implies that co-reductions of GHG emissions (e.g., CO_2 and CH_4 emission reductions from an early retirement of a coal-fired power plant (e.g., Tanaka et al., 2019)) are not explicitly considered in our MAC curve approach. The third assumption implies that GHG abatements occur exclusively in each region without relying on other regions. The validity of these assumptions can be seen in Section 4. Additional conditions were applied to derive MAC curves from each model, as summarized in Table 1. These conditions were identified based on visual inspection of the data from each IAM.

Deleted: more

Deleted: can be seen in Table S2

Deleted: did

Deleted: 3 MAC curves emulating IAMs

Deleted: year

Deleted: the

Deleted: term

Deleted: the fractional term

Deleted: 0%

Deleted: .

Deleted: turns

Deleted: mitigation scenarios.

Deleted: We then fitted a mathematical function $f(x)$ (equation (1); selected among several others as explained below) as a MAC curve to capture the emission abatement level for a given carbon price. We used a common time-invariant functional form of equation (1) for all cases (i.e., models, gases, regions, sources, and portfolios) for consistency, comparability, and simplicity of use.

$$f(x) = a * x^b + c * x^d \quad (1)$$

a, b, c, and d are the parameters to optimize for each case. x is a variable representing the emission abatement level in percentage relative to the assumed baseline level. The carbon price is in per ton of CO_2-equivalent emissions, in which GWP100 (28 and 265 for CH_4 and N_2O, respectively (IPCC, 2013)) is used to convert to the prices of CH_4 and N_2O, as assumed in the IAMs emulated here (Harmsen et al., 2016). GWP100 is practically a default emission metric used to convert non-CO_2 GHG emissions to the common scale of CO_2, which has been used for decades in multi-gas climate policies and assessments including the Paris Agreement (Lashof and Ahuja, 1990; Fuglestvedt et al., 2003; Tanaka et al., 2010; Tol et al., 2012; Levasseur et al., 2016; UNFCCC, 2018). MAC curves were obtained from the data for the period 2020-2100. There are three key assumptions in our approach: i) MAC curves are assumed time-independent, ii) abatement levels are assumed independent across gases, and iii) abatement levels are assumed independent across regions. While MAC curves are more commonly time-dependent or for a specific point in time, time-independent MAC curves have also been used for long-term pathway calculations (Johansson et al., 2006; Tanaka and O'Neill, 2018; Tanaka et al., 2021) and shorter-term assessments (De Cara and Jayet, 2011). The implications of the first assumption will be discussed later in this section. The second assumption indicates that co-reductions of GHG emissions (e.g., emission abatement of CO_2 and CH_4 from an early retirement of a coal-fired power plant (e.g. Tanaka et al., 2019)) are not explicitly considered in our MAC curve approach. The third assumption implies that the regional distribution of GHG abatements is determined primarily by the global cost-effectiveness (Su et al., 2022). The validities of these assumptions can be seen in Section 4, in which MAC curves are combined with a simple climate model to reproduce original IAM outcomes. There are further conditions applied to derive MAC curves from each model as summarized in Table 1. These conditions were identified based on visual inspection of data from each IAM.

Model	Label	Solution concept	Solution method	Spatial resolution	Gas	Range of carbon budget ($GtCO_2$)	Number of scenarios	Data range for MAC curve fitting
AIM/CGE V2.2	AIM	General equilibrium	Recursive dynamic	Global Regional	CO_2 CH_4 N_2O	300-1,800	34	Carbon prices lower than \$110/tCO_2 before 2040 and all data after 2040
COFFEE 1.1	COFFEE	Partial equilibrium	Intertemporal optimization	Global Regional	CO_2 CH_4 N_2O	400-2,500	52	Carbon prices lower than \$50/tCO_2 with abatement levels below 100% under scenarios without negative emissions
GEM-E3 V2021	GEM	General equilibrium	Recursive dynamic	Global Regional	CO_2 CH_4 N_2O	400-1,800	23	All scenarios
IMAGE 3.0	IMAGE	Partial equilibrium	Recursive dynamic	Global Regional	CO_2 CH_4 N_2O	600-3,000	21	All data except: EN_INDCi2030_800f, EN_NPi2020_600f, EN_INDCi2030_1000f, EN_Npi2020_800
MESSAGEix-GLOBIOM 1.1	MESSAGE	General equilibrium	Intertemporal optimization	Global Regional	CO_2 CH_4 N_2O	200-3,000	52	All scenarios except: EN_NPi2020_450, EN_NPi2020_500
POLES-JRC ENGAGE	POLES	Partial equilibrium	Recursive dynamic	Global	CO_2 CH_4 N_2O	300-3,000	53	Carbon price below \$1,000/tCO_2 before 2050 and below \$5,000/tCO_2 thereafter
REMIND-MAgPIE 2.1-4.2	REMIND	General equilibrium	Intertemporal optimization	Global	CO_2 CH_4 N_2O	200-3,000	58	All scenarios except: EN_INDCi2030_700, EN_INDCi2030_800, EN_NPi2020_400, EN_NPi2020_500
TIAM-ECN 1.1	TIAM	Partial equilibrium	Intertemporal optimization	Global	CO_2 CH_4 N_2O	800-3,000	35	All scenarios
WITCH 5.0	WITCH	General equilibrium	Intertemporal optimization	Global	CO_2 CH_4 N_2O	400-3,000	51	All scenarios
GET 10.0	GET	Partial equilibrium	Intertemporal optimization	Global	Energy CO_2	-	22	Carbon prices lower than \$5,000/tCO_2; excluded data for very high abatements with disproportionally low costs (found typically after 2100)

Table 1. Models and data considered for emIAM. This table describes the features of models (including the versions used) and the data (gases, regions (ten regions)) that were used to derive our MAC curves. "Solution concept" and "solution method" for ENGAGE IAMs (first nine IAMs in the table) are based on Riahi et al. (2021), Guivarch et al. (2022), and IAMC_wiki (2022). Total anthropogenic

Deleted: captured by
Deleted: curves
Inserted Cells
Inserted Cells
Deleted: …
Inserted Cells
Inserted Cells
Deleted: data
Deleted:
Deleted:
Deleted:
Deleted: data
Deleted: prices lower than
Deleted: data
Deleted:
Deleted:
Deleted:
Deleted: data
Deleted: data
Deleted: 1.
Deleted: 10

(and separately energy-related and non-energy-related) CO_2, CH_4, and N_2O emissions were taken from ENGAGE IAMs; only energy-related CO_2 emissions were used from GET.

Deleted:

We fit a mathematical function $f(x)$ to the data from each IAM as a MAC curve to capture the emission abatement level for a given carbon price. In selecting the functional form of MAC curves, we had to balance the competing requirements of i) capturing complex nonlinear relationships between the carbon price and the abatement level and ii) keeping the functional form at low complexity. We therefore tested the performance of several functional forms to fit the data, some of which were based on previous studies (Johansson, 2011; Su et al., 2017; Tanaka and O'Neill, 2018). The candidate functions are summarized in Table S2, along with the ranges of parameters considered. To infer a good functional form, we further tried the symbolic regression approach by using the software HeuristicLab, but we were unable to obtain a functional form that is more satisfactory than those suggested in Table S2. Our results indicated that the polynomial function with two algebraic terms (equation (1)) gave the highest r^2 and adjusted r^2 among the equations tested in more than 50% of the cases, consistently performing best for all IAMs (see the Zenodo repository and Table S3). A polynomial function with only one algebraic term is insufficient: two distinct algebraic terms are generally needed to capture the trend of our data (sometimes with a kink like a "reversed L" shape or with a plateau as shown later).

Therefore, we used a common functional form of equation (1) to generate MAC curves for all cases (i.e., models, gases, regions, and sources in ENGAGE IAMs and portfolios in GET) for consistency, comparability, and simplicity of use.

$$f(x) = a * x^b + c * x^d \quad (1)$$

a, b, c, and d are the parameters to be optimized in each case. x is the variable representing the emission abatement level in percentage relative to the assumed baseline level. The carbon price (i.e., $f(x)$ in equation (1)) is expressed in per ton of CO_2-equivalent emissions, using GWP100 (28 and 265 for CH_4 and N_2O, respectively (IPCC, 2013)) to convert CH_4 and N_2O emissions, as assumed in the IAMs emulated here (Harmsen et al., 2016). GWP100 is effectively the default emission metric used to convert non-CO_2 GHG emissions to the common scale of CO_2 and has been used for decades in multi-gas climate policies and assessments, including the Paris Agreement (Lashof and Ahuja, 1990; Fuglestvedt et al., 2003; Tanaka et al., 2010; Tol et al., 2012; Levasseur et al., 2016; UNFCCC, 2018, 2023).

In addition to deriving the MAC curves, we derived the maximum abatement level from each IAM, which reflected, for example, the limit of CCS capacity and hard-to-abate sectors. The minimum abatement level is, by definition, zero in all simulation periods, unless there is inter-sectoral emission trading that can increase emissions. We also estimated upper limits of the first and second derivatives of temporal changes in abatement levels, which account for the limits of the rate of technological change and the socio-economic inertia (e.g., barriers to the diffusion of new technologies (Schwoon and Tol, 2006)), respectively. The limits on the first and second derivatives of abatement changes will prohibit the use of deep mitigation levels in the MAC curve in early periods. These barriers to rapid emission reductions and the associated costs could also be introduced by more complex functional forms internally in the MAC curves (Ha-Duong et al., 1997; Schwoon and Tol, 2006; De Cara and Jayet, 2011; Hof et al., 2021), but we applied such limits externally on the MAC curves. "Learning by doing" and "learning with time," which reduce the mitigation cost with abatement (endogenously) and time (exogenously), respectively

Deleted: for fitting
Deleted: (i.e., equation (1)),
Deleted: needed
Deleted: for
Deleted: Therefore, we
Deleted: for fitting
Deleted: . The candidate functions
Deleted: are
Deleted: ,
Deleted: S1,
Deleted: not able
Deleted: for our purpose.
Deleted: R^2
Deleted: R^2
Deleted: for
Deleted: performing
Deleted: the
Deleted:). Therefore, we applied equation (1) to generate MAC curves.…
Deleted: was
Deleted: were
Deleted: It should be noted that we do not consider the parametric uncertainties in individual MAC curves, but
Deleted: use
Deleted: MAC curves from multiple
Deleted: can provide a sense
Deleted: model uncertainties.
Deleted: derivation of
Deleted: for each IAM from its simulation results under all carbon budgets or carbon prices
Deleted: .
Deleted: calculated for each gas and each IAM the maximum…
Deleted: corresponded roughly to
Deleted: limit
Deleted: rate
Deleted: ,
Deleted: can prevent
Deleted: limits
Deleted: also
Deleted: externally
Deleted: reduces
Deleted: ,

(Hof et al., 2021), are not explicitly considered in our MAC curve approach, but are partially captured in our approach, which describes percentage reduction rates relative to rising baseline scenarios. For example, constant emission reductions in absolute terms can appear smaller over time in relative terms and thus become less costly in our approach.

For each IAM, we computed the rate of change in the abatement level at each time step from the previous time step (i.e., first derivatives) over the entire available period. We then approximated such data with a log-normal distribution and assumed the three-sigma level (upper side) as the maximum of the first derivative of abatement changes. Likewise, we computed the rate of change of the rate of change in the abatement level (i.e., second derivatives), approximated the data with a normal distribution, and assumed the three-sigma level (upper side) as the maximum of the second derivative of abatement changes. We further assumed that the minimum of the first and second derivatives were at the opposite sign of the maximum of the first and second derivatives, respectively. These limits are applied when MAC curves are coupled with ACC2 to generate cost-effective pathways (Section 4).

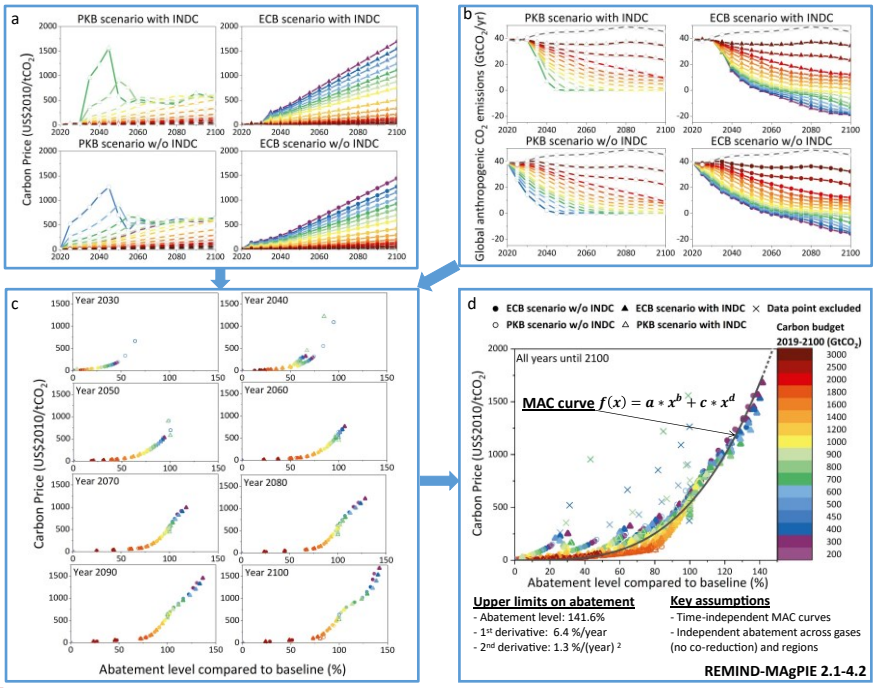

Figure 1. Overview of the methods to derive MAC curves and limits on abatement (upper limits on abatement levels and their first and second derivatives). The figure uses the data for global total anthropogenic CO_2 emissions from REMIND for illustration. The chromatic colors indicate the respective carbon budgets for the period 2019 – 2100 in $GtCO_2$. The gray color indicates the baseline scenario ("NPi2100" in the original scenario name). Scenarios without INDC consider currently implemented national policies (circle; indicated as "NPi2020" in the original scenario name); scenarios with INDC further consider national emission pledges until 2030

Deleted: in part, albeit unintended,
Deleted: that
Deleted: (until 2080).
Deleted: the
Deleted: term
Deleted: with
Deleted: the percentage term
Deleted: expensive
Deleted: each gas and
Deleted: for each gas and each IAM
Deleted: signs
Deleted: will be
Deleted:
Deleted: 1.
Deleted: as an example. Scenario names
Deleted: cumulative
Deleted: NPi2020 scenarios
Deleted:); INDCi2030

(triangle; indicated as "INDCi2030" in the original scenario name). ECB scenarios consider carbon budgets till the end of this century, with a possibility of temporal budget overspending (filled circles; with "f" in the original scenario name); PKB scenarios consider carbon budgets without allowing temporal budget overspending (open circles; without "f" in the original scenario name). Crosses indicate data points from scenarios that were not considered in the derivation of the MAC curve (i.e., EN_INDCi2030_700, EN_INDCi2030_800, EN_NPi2020_400, and EN_NPi2020_500 for REMIND (see Table 1)). In the equation of the MAC curve, a, b, c, and d are the parameters to be optimized; x is the variable representing the abatement level in percentage relative to the assumed baseline level. Note that panel c shows data only for every ten years for the sake of presentation.

In summary, we combined a MAC curve with the upper and lower limits on abatement levels and their first and second derivatives to emulate the behavior of an IAM, as illustrated in Figure 1 using the output from REMIND as an example (corresponding figures for AIM and MESSAGE in Figures S1 and S2 of Supplement). The upper two panels show the original data from REMIND: the carbon price pathways corresponding to the series of carbon budgets (Figure 1a) and the global anthropogenic CO_2 emissions (Figure 1b) from the four types of scenarios (ECB scenarios without INDC, ECB scenarios with INDC, PKB scenarios without INDC, and PKB scenarios with INDC). These data are rearranged to show the relationship between the carbon price and the abatement level in percentage relative to baseline every ten years (original data every five years before 2060) (Figure 1c). In the near term, data points can only be seen at low abatement levels. With time, data points proceed to deeper abatement levels. Taken together over all years, Figure 1d shows a secular relationship, providing a basis for a time-independent MAC curve. The stable MAC curve is an interesting finding in itself because, despite the presence of time-dependent processes in this intertemporal optimization model (Campiglio et al., 2022), the same relationship persists over time between the carbon price and the abatement level. But why does this time-independent approach work so well to capture IAMs that include time-dependent processes? The use of percentage reductions in our MAC curve approach goes some way to explaining this. Since most of the baseline scenarios are rising as noted above, the same amount of emission abatement in absolute terms can become smaller with time in percentage terms, which inadvertently but effectively captures "learning by doing" and "learning with time". When the underlying data are presented in absolute terms, the data distribution appears more dispersed (Figure S3 for AIM, MESSAGE, and REMIND). Outliers arising from very low carbon budget scenarios (crosses in Figure 1d) were identified and manually excluded from the derivation of the MAC curve (Table 1), although excluding such scenario(s) limits the range of applicability of the MAC curve.

3.2 MAC curves from ENGAGE IAMs

3.2.1 Carbon price and abatement level

Figure 2 shows the relationships between the carbon price and the abatement level for global total anthropogenic CO_2 emissions obtained from nine ENGAGE IAMs. Overall, the relationships between the carbon price and the CO_2 abatement level are well captured by time-independent MAC curves for most IAMs here. The results vary in terms of the range of carbon prices, the range of abatement levels, and the dispersion of data points. For example, the carbon prices of AIM and COFFEE remain

Deleted:). Among NPi2020 scenarios, those with "f" are net-negative emissions scenarios

Deleted:); those without "f" are net-zero CO_2 emissions scenarios

Deleted: .

Deleted: optimize

Deleted: (i.e., NPi2100 (not shown)).

Deleted: Figure 1 illustrates the approach described above by using the output from REMIND as an example (corresponding figures for AIM and MESSAGE in Figures S1 and S2 of Supplement (note: figures and tables with "S" in numbering are in Supplement)).

Deleted: sum

Deleted: .

Deleted: series of

Deleted: in Figure 1

Deleted: at each point in time (

Deleted:) as obtained from REMIND simulated with

Deleted: range of carbon budgets. Data

Deleted: only

Deleted: in the near-term.

Deleted: Putting

Deleted: across

Deleted: the right panel of

Deleted: 1

Deleted: which allows us to approximate with

Deleted: Even though there are

Deleted: due to technological changes and socio-economic inertia …

Deleted: ,

Deleted: can apply

Deleted: There are outliers arising from very low carbon budget scenarios (crosses in the right panel of Figure 1). To…

Deleted: IAM processes collectively

Deleted: are

Deleted: in

Deleted: pointed out earlier

Deleted: the

Deleted: term

Deleted: the

Deleted: term

Deleted: ," at least partially. If

Deleted: shown

Deleted: the

Deleted: term

Deleted: does appear

Deleted: Figures

Deleted: -S5

Deleted: differ

Deleted: stay

below $500/tCO$_2$, while the carbon prices of POLES and MESSAGE can exceed $5,000/tCO$_2$. The maximum abatement levels of COFFEE and REMIND are over 150%, while others are in the range of 100%-120%. AIM provides a limited amount of data at low abatement levels. IMAGE and POLES produce more dispersed data distributions than other models, which may be related to the fact that these models are recursive dynamic models (Table 1); however, the other recursive dynamic models, AIM and GEM, produce less dispersed data distributions that can be well captured by MAC curves. POLES can be seen as an example where our time-independent MAC curve approach does not work well. The MAC curve, if taken every five years, shifts to the right over time (Figure S4). Visual inspection of the data distributions reveals little difference between the ECB scenarios and PKB scenarios (except for WITCH), indicating that the MAC curves are generally consistent for both types of scenarios in these IAMs. Results for other gases and for energy-related emissions are shown in Figures S5-S36.

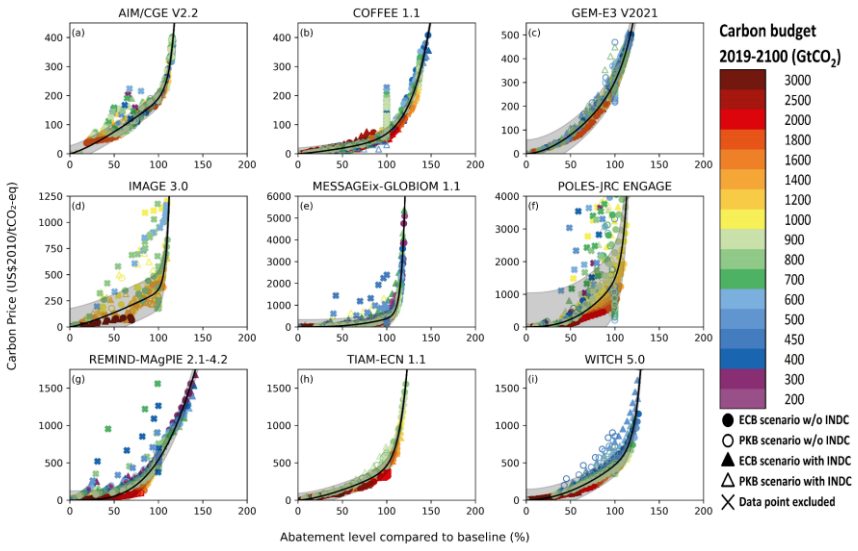

Figure 2. Relationships between the carbon price and the global total anthropogenic CO_2 abatement level obtained from nine ENGAGE IAMs. Each panel shows the results from each ENGAGE IAM. Data were obtained from the ENGAGE Scenario Explorer and are shown in colors and markers as designated in the legend. Black lines are the MAC curves. Crosses are the data points that were not included in the derivation of MAC curves (Table 1). The shaded bands are the 95% confidence intervals of the fitted curves calculated by $\hat{y} \mp t_{\frac{\alpha}{2}} * S_\varepsilon * \sqrt{1+\frac{1}{n}+\frac{(x-\bar{x})^2}{\sum x^2-\frac{(\sum x)^2}{n}}}$ (Thomson and Emery, 2014), where $S_\varepsilon = \sqrt{\frac{\sum(y-\hat{y})^2}{n-2}}$, n is the sample size, $t_{\frac{\alpha}{2}}$ is the critical value of t-distribution, $\bar{x}$ is the mean of samples, $\hat{y} = f(x)$, and x, y are the original abatement level and carbon price result from the IAM, respectively.

Deleted: above
Deleted: offers
Deleted: in the near term.
Deleted: give
Deleted:). However,
Deleted: , which
Deleted: Nevertheless, on the whole, the relationships between the carbon price and the CO_2 abatement level are well captured by
Deleted: curves for most IAMs here.
Deleted: differences
Deleted: net-negative emissions
Deleted: net-zero CO_2 emissions
Deleted: valid
Deleted: . If we consider
Deleted: terms of the absolute amount of abatement, instead of percentage abatement, the data distributions become more dispersed (Figure S3-S5).
Deleted: can be found
Deleted: S6-S37

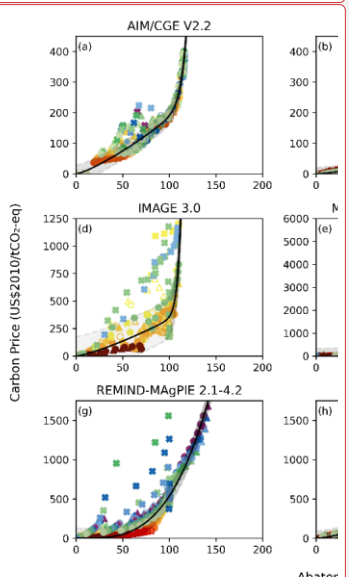

Deleted:
Deleted: 2.
Deleted: considered in the derivation of MAC curves (Table 1).…

3.2.2 First and second derivatives of abatement changes

The first and second derivatives of temporal changes in abatement levels for global total anthropogenic CO_2 emissions from each ENGAGE IAM are shown in Figure 3. Data for the first derivatives primarily distribute on the positive side and can be best captured by log-normal distributions, among other distributions tested. On the other hand, data for the second derivatives spread on both the positive and negative sides and can be approximated by normal distributions. Based on visual inspection, we found that three-sigma ranges of distributions can largely capture data ranges. We therefore use three-sigma ranges as the limits on the first and second derivatives of abatement changes. There are outliers (now shown) originating from PKB scenarios, which we speculate are caused by sudden declines in carbon prices around the period of achieving net zero CO_2 emissions (Figure SI 1.1-6 of Riahi et al. (2021)). These outliers were effectively removed by considering three-sigma ranges (rather than the maxima and minima of the original data points). For other gases and for energy-related emissions, see Figures S38-S87.

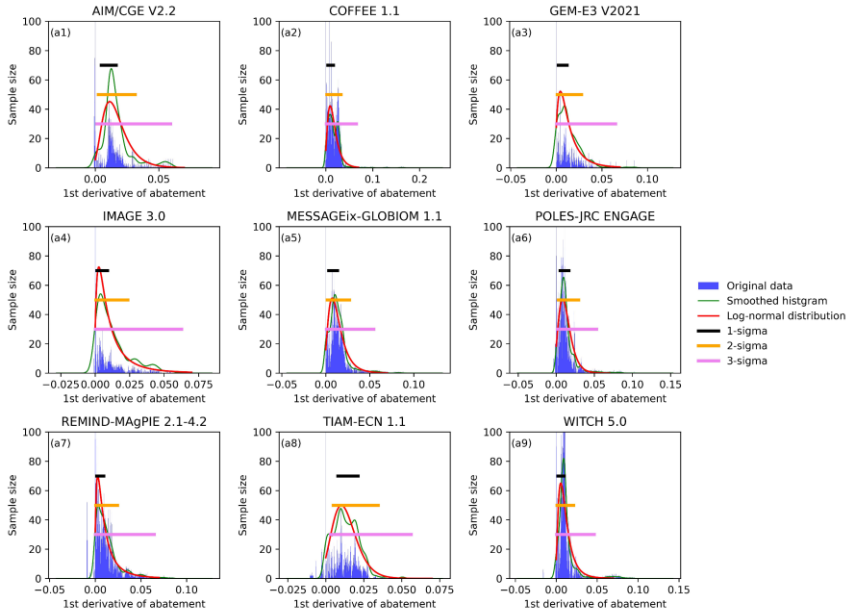

Deleted: On the basis of

Deleted: thus

Deleted: net-zero CO_2 emissions

Deleted: drops

Deleted: S40

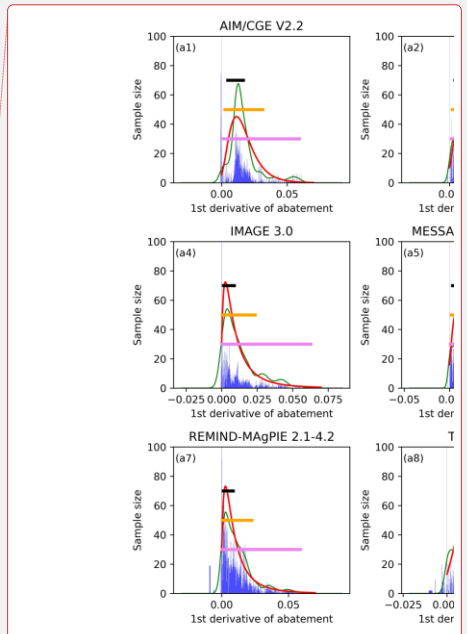

Deleted: ...

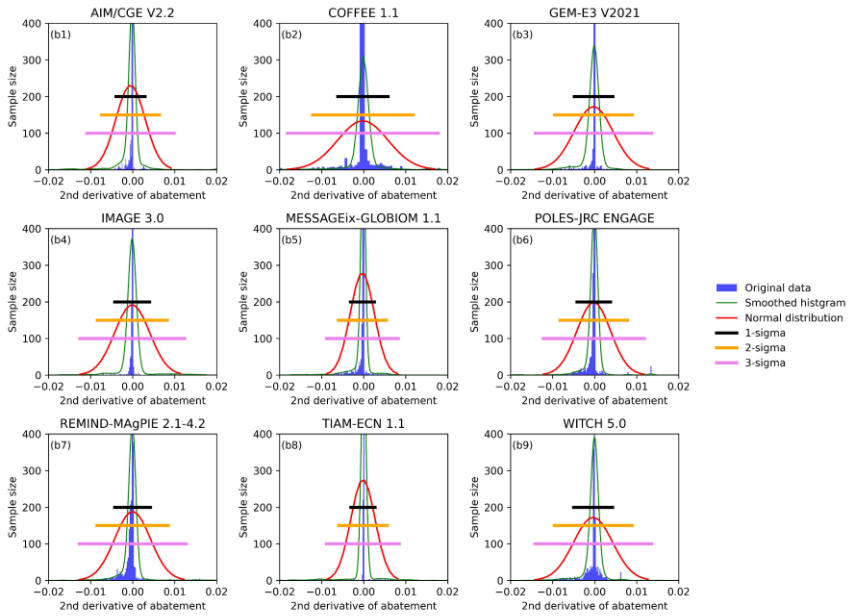

Figure 3. The first and second derivatives of temporal changes in abatement levels for the global total anthropogenic CO_2 emissions from each ENGAGE IAM. A log-normal distribution is applied to the data for the first derivatives of abatement changes obtained from each IAM. A normal distribution is applied to the data for the second derivatives of abatement changes obtained from each IAM.

The upper limits on the first and second derivatives of abatement changes estimated for ENGAGE IAMs are summarized in Table 2. Those for ACC2 were assumed to be 4.0 %/year and 0.4 %/(year)^2, respectively, for all three gases (CO_2, CH_4, and N_2O) (Tanaka and O'Neill, 2018; Tanaka et al., 2021). ENGAGE IAMs give higher upper limits on the first and second derivatives than ACC2 for CO_2. For the other two gases, ENGAGE IAMs also give higher upper limits on the second derivatives but tend to indicate lower upper limits on the first derivatives.

The upper limits on the first and second derivatives of CO_2 abatement can determine the earliest possible year of achieving net zero CO_2 emissions (i.e., 100% abatement) for each IAM. In the case of ACC2, it is the year 2050 when net zero CO_2 emissions become first possible, if the abatement can start in 2020. Figure S88 compares the earliest possible net zero years implied by the upper limits on the first and second derivatives with the years of net zero in carbon budget scenarios from each ENGAGE IAM. The figure shows that the former precedes the latter in all IAMs, indicating that the upper limits based on three-sigma ranges are large enough to allow pathways to achieve net zero as shown by each IAM.

Deleted: 3.

Deleted: (%/

Deleted: available

3.2.3 Global MAC curves

Figure 4 shows the global MAC curves for total anthropogenic and energy-related CO_2, CH_4, and N_2O emissions from nine ENGAGE IAMs and other studies. The parameter values of these global MAC curves and associated limits on abatement are shown in Table 2 (for total anthropogenic emissions) and Table S4 (for energy-related emissions).

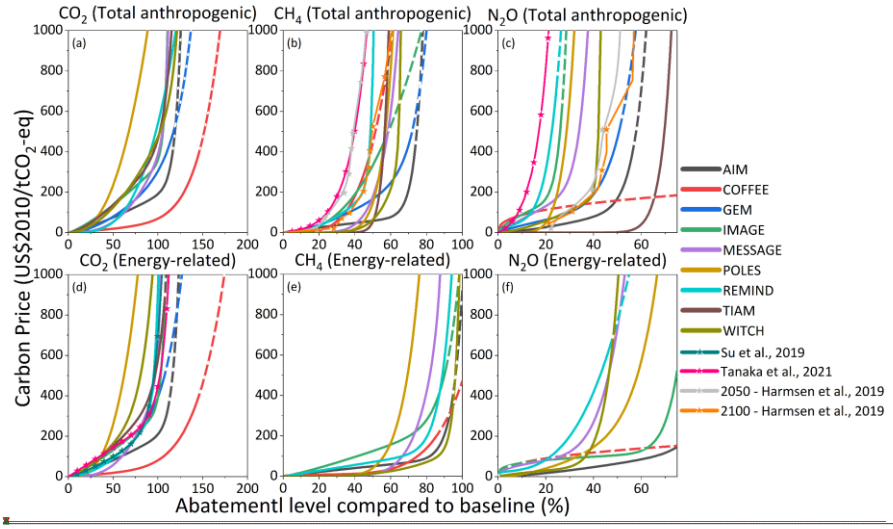

Figure 4. Global MAC curves for total anthropogenic and energy-related CO_2, CH_4, and N_2O emissions derived from nine ENGAGE IAMs. In panels (a) to (f), the solid line indicates that the MAC curve is within the applicable range; the dashed line means that it is outside the applicable range (i.e., above the maximum abatement level indicated from underlying IAM simulation data or above the range of carbon prices considered for fitting the MAC curve; see Tables 1 and 2). Different colors indicate different IAMs. The MAC curves from selected previous studies (Su et al., 2017; Harmsen et al., 2019; Tanaka et al., 2021) are shown for comparison. The MAC curves from Harmsen et al., (2019) are time-dependent and the figure shows those for the years 2050 and 2100.

Model	Gas	*a*	*b*	*c*	*d*	MaxABL	Max1st	Max2nd
AIM	CO_2	182.14	1.27	8.68	19.71	116.2	5.9	1.0
	CH_4	108.99	0.91	78686	17.91	73.6	6.1	1.3
	N_2O	282.34	1.46	243642	11.84	56.1	4.5	1.0
COFFEE	CO_2	46.66	1.29	22.59	7.01	147.2	6.5	1.8
	CH_4	3658.91	4.05	3658.91	4.05	47.7	2.3	1.3
	N_2O	102.75	0.37	102.75	0.37	20.2	3.9	1.4
GEM	CO_2	267.14	1.76	36.85	8.53	118.2	6.5	1.4
	CH_4	486.16	1.59	7133.48	10.70	72.0	4.6	1.1

Deleted: .
Deleted: S3
Moved down [2]: **Global MAC curves for total anthropogenic and energy-related CO_2, CH_4, and N_2O emissions derived from nine ENGAGE IAMs.** In panels (a) to (f), the solid line indicates that the MAC curve is within the applicable range; the dashed line means that it is outside the applicable range (i.e., above the maximum abatement level indicated from underlying IAM simulation data or above the range of carbon prices considered for fitting the MAC curve; see Tables 1 and 2). Different colors indicate different IAMs.
Moved down [3]: MAC curves for total anthropogenic and energy-related CO_2 emissions resemble each other since total anthropogenic CO_2 emissions are predominantly energy-related CO_2 emissions. COFFEE gives the lowest carbon prices among all IAMs over a wide range of abatement levels; POLES shows the highest carbon prices. AIM has the second-lowest carbon prices at
Moved down [4]: CH_4 MAC curves generally rise sharply at lower abatement levels than CO_2 MAC curves. All MAC curves for energy-related CH_4 emissions are low up to about 50% abatement level, presumably reflecting low-cost abatement opportunities. AIM and WITCH give a low carbon price up to 80-90% abatement level for energy-related CH_4 emissions. Due to limited N_2O abatement opportunities, N_2O MAC curves rise steeply at low abatement levels, with the one from REMIND rising earliest.
Deleted: …
Deleted:
Deleted: the abatement level of 63% and beyond. …
Moved (insertion) [2]
Deleted: …
Deleted: 146.7
Deleted: 1
Deleted: 0
Deleted: 0
Deleted: 1
Deleted: 6
Deleted: 3
Deleted: 1
Deleted: 1
Moved down [6]: 7133.48
Moved down [8]: 10.70
Moved up [5]: 486.16
Moved up [7]: 1.59
Moved (insertion) [5]
Moved (insertion) [7]
Moved (insertion) [6]
Moved (insertion) [8]
Deleted: 71.9
Deleted: 3
Deleted: 0.9

	N_2O	240.14	0.83	31072	6.54	51.1	4.0	0.9
IMAGE	CO_2	330.58	1.27	28.57	29.83	110.1	6.3	1.2
	CH_4	959.11	2.53	959.11	2.53	58.3	3.1	0.6
	N_2O	426.52	0.68	1.54*10^8	9.70	26.3	2.4	0.5
MESSAGE	CO_2	368.79	2.78	18.30	30.24	120.9	5.4	0.8
	CH_4	16789	6.57	3.29*10^7	29.08	73.3	3.5	0.6
	N_2O	610.67	0.97	7909596	9.47	45.2	1.9	0.3
POLES	CO_2	1347.98	2.52	144.57	21.87	147.1	5.3	1.2
	CH_4	48160	9.36	48160	9.36	75.9	4.3	1.0
	N_2O	1512842	6.42	1513291	94.73	37.3	2.3	0.5
REMIND	CO_2	269.52	3.38	269.52	3.38	136.2	5.9	1.0
	CH_4	1002.16	2.11	1.61*10^11	28.11	51.2	3.4	1.2
	N_2O	224.21	0.65	633401	4.92	24.8	1.6	1.0
TIAM	CO_2	384.32	1.48	78.52	13.31	121.7	5.6	0.9
	CH_4	1.23*10^7	17.81	157.83	100	59.5	3.9	1.0
	N_2O	215121	16.79	99.08	100	73.3	4.3	2.3
WITCH	CO_2	462.12	1.89	10.13	18.05	128.2	4.7	1.4
	CH_4	6658.29	6.72	2.78*10^15	69.59	66.7	3.7	2.1
	N_2O	681.73	1.52	9.10*10^18	43.78	42.8	3.1	1.1

Table 2. Parameter values of global MAC curves for total anthropogenic CO_2, CH_4, and N_2O emissions derived from nine ENGAGE IAMs and associated limits on abatement. See equation (1) for parameters a, b, c, and d. MaxABL denotes the maximum abatement level (%) of each gas indicated from IAM simulation data. The units for a and c are US$2010/t$CO_2$. Max1st and Max2nd represent the maximum first and second derivatives (%/year and %/(year)^2), respectively, of abatement changes of each gas also derived from IAM simulation data. For those of global MAC curves for energy-related CO_2, CH_4, and N_2O emissions, see Table S4. For those of regional MAC curves, see the Zenodo repository.

MAC curves for total anthropogenic and energy-related CO_2 emissions resemble each other since total anthropogenic CO_2 emissions are predominantly energy-related CO_2 emissions. COFFEE gives the lowest carbon prices among all IAMs over a wide range of abatement levels; POLES shows the highest carbon prices. AIM has the second-lowest carbon prices at abatement levels of 63% and above. REMIND gives higher carbon prices than AIM above the abatement level of 60%. The functional form of the MAC function used by Su et al. (2017) is consistent with our study, and Tanaka et al. (2021) used equation (2) in Table S2. Harmsen et al. (2019) considered time-dependent MAC curves and no explicit function is provided. Despite some differences in the form of the functions, the MAC curves for energy-related CO_2 used in Su et al. (2017) and Tanaka et al. (2021) are within the range of the MAC curves from ENGAGE IAMs, but the MAC curves for CH_4 and N_2O used in Tanaka et al. (2021) show a higher level of marginal carbon price. Harmsen et al. (2019) show that CH_4 MAC curve in 2050 is also to the left of our results, but that in 2100 are close to our study. Meanwhile, their results for N_2O are in the middle of our results and not much different between 2050 and 2100.

The difference between MAC curves for total anthropogenic and energy-related emissions is more pronounced for CH_4 and N_2O than for CO_2 because of greater mitigation opportunities outside of the energy sector. CH_4 MAC curves generally rise sharply at lower abatement levels than CO_2 MAC curves. All MAC curves for energy-related CH_4 emissions are low up

Deleted: 3.8
Deleted: 7
Moved down [10]: 28.57
Moved down [12]: 29.83
Moved up [9]: 330.58
Moved up [11]: 1.27
Moved (insertion) [9]
Moved (insertion) [11]
Moved (insertion) [10]
Moved (insertion) [12]
Moved down [15]: 9.70
Moved up [13]: 426.52
Moved up [14]: 0.68
Moved (insertion) [13]
Moved (insertion) [14]
Moved (insertion) [15]
Deleted: 1.54E+08
Moved down [17]: 18.30
Moved down [19]: 30.24
Moved (insertion) [16]
Moved (insertion) [18]
Moved (insertion) [17]
Moved up [16]: 368.79
Moved up [18]: 2.78
Moved (insertion) [19]
Moved up [20]: 16789
Moved up [21]: 6.57
Moved (insertion) [20]
Moved (insertion) [21]
Deleted: 3.29E+07
Deleted: 29.08
Deleted: 131.9
Deleted: 4.8
Deleted: 0.9
Deleted: 7
Deleted: 2
Deleted: .9
Moved (insertion) [22]
Moved down [23]: 1513291
Moved down [25]: 94.73
Moved (insertion) [24]
Moved (insertion) [23]
Moved up [22]: 1512842
Moved (insertion) [25]
Moved up [24]: 6.42
Deleted: 2
Moved up [26]: 1002.16
Moved (insertion) [26]
Deleted: 1.61E+11
Deleted: 28
Deleted: 2
Moved (insertion) [27]
Moved (insertion) [29]

to about 50% abatement level, presumably reflecting low-cost abatement opportunities. AIM and WITCH give a low carbon price up to 80-90% abatement level for energy-related CH_4 emissions. Due to limited N_2O abatement opportunities, N_2O MAC curves rise steeply at low abatement levels, with the one from REMIND rising earliest.

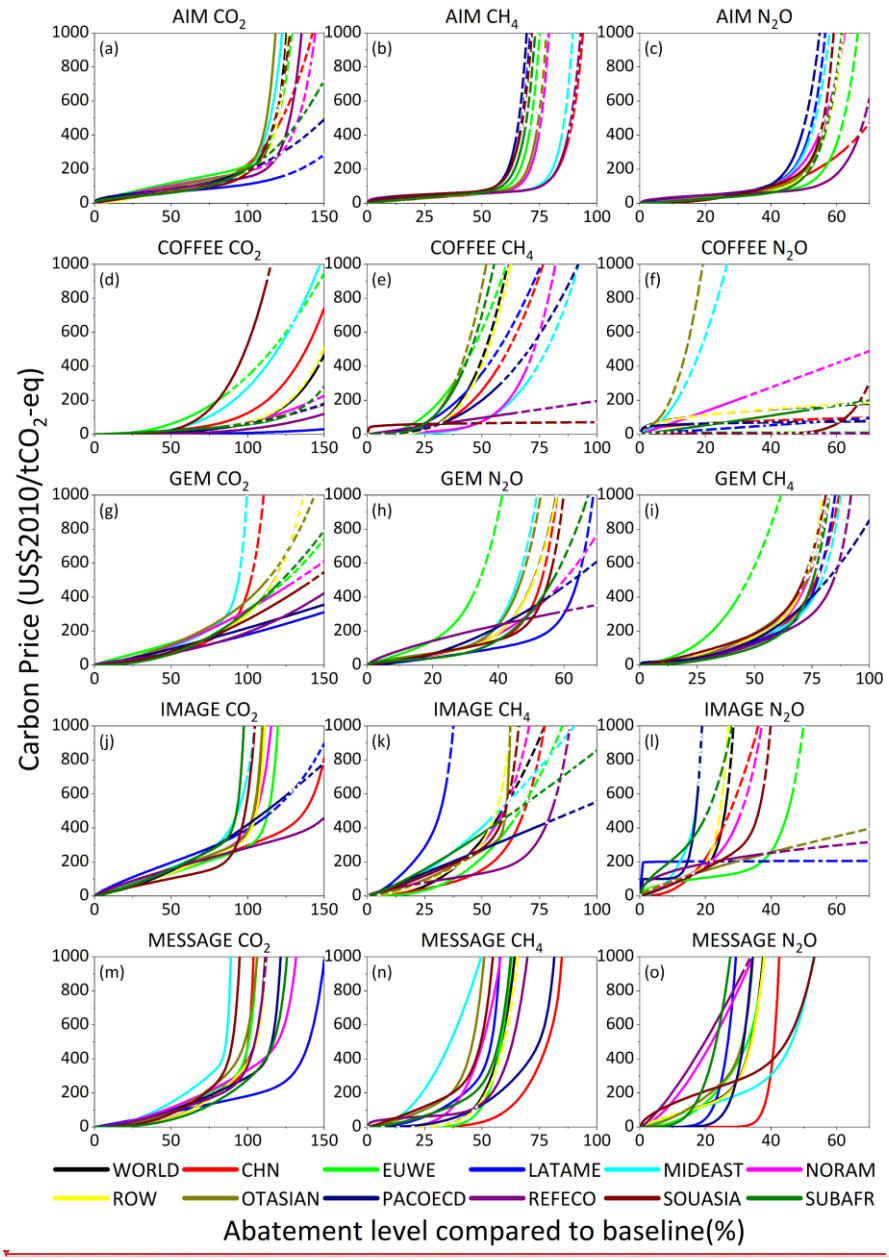

Figure 5. Regional MAC curves for total anthropogenic CO_2, CH_4, and N_2O emissions derived from five ENGAGE IAMs. The

Deleted:

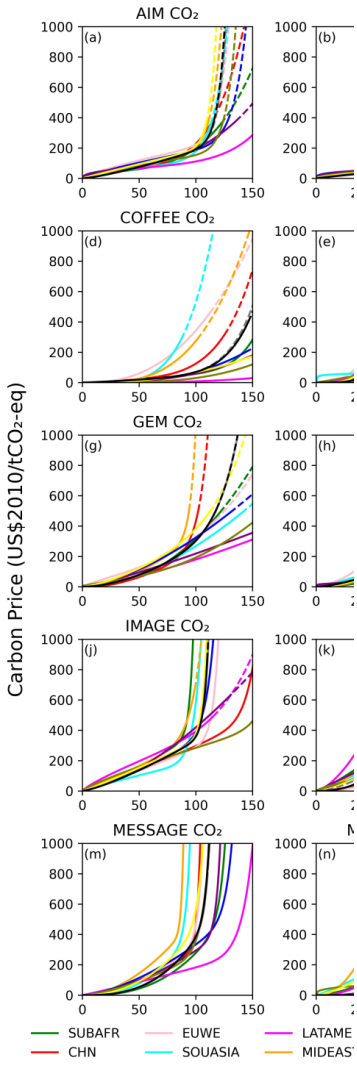

Deleted: 5.

solid line indicates that the MAC curve is within the applicable range; the dashed line means that it is outside the applicable range (i.e., above the maximum abatement level indicated from underlying IAM simulation data or above the range of carbon prices considered for fitting the MAC curve; see Tables 1 and 2). Different colors indicate different regions: China (CHN), European Union and Western Europe (EUWE), Latin America (LATAME), Middle East (MIDEAST), North America (NORAM), Other Asian countries (OTASIAN), Pacific OECD (PACOECD), Reforming Economies (REFECO), South Asia (SOUASIA), Sub-Saharan Africa (SUBSAFR), and Rest of World (ROW).

3.2.4 Regional MAC curves

Figure 5 shows the regional MAC curves for total anthropogenic CO_2, CH_4, and N_2O emissions from five ENGAGE IAMs. The parameter values of the regional MAC curves and associated limits on abatement can be found in our Zenodo repository. While various inter-model and inter-regional differences can be seen in Figure 5, the regional variations of the AIM MAC curves appear to be the smallest for all three gases.

MIDEST generally shows a high CO_2 MAC curve relative to other regions. LATAM gives the lowest MAC curve at abatement levels above approximately 79% in all IAMs considered here, except for the IMAGE model with SOUASIA and REFECO being the lowest MAC curve at abatement levels of above and below 90%, respectively. LATAM also indicates very deep CO_2 abatement potentials exceeding 150% in some models. AIM's CH_4 MAC curves indicate low-cost CH_4 abatement opportunities up to abatement levels of approximately 50% in all regions, while such opportunities appear less abundant in the CH_4 MAC curves from other models. REFECO exhibits a very low CH_4 MAC curve in all five models. MIDEST gives either a high or a low CH_4 MAC curve, depending on the IAM. The N_2O MAC curves generally rise sharply earlier than the CH_4 MAC curves.

3.3 MAC curves from GET

Figure 6 shows the relationships between the carbon price and the abatement level of global energy-related CO_2 emissions and their dependency on the underlying technology portfolios considered in GET. MAC curves from different technology portfolios are compared in Figure 7. They are further compared with the global MAC curves for energy-related CO_2 emissions from ENGAGE IAMs and other studies. The parameter values of these global MAC curves and associated limits on abatement are shown in Table 3. Further details of the first and second derivatives of abatement changes from GET can be found in Figures S38 and S39.

Deleted:
Deleted: look
Deleted: the
Deleted: level
Deleted: The
Deleted: from AIM
Deleted: Global
Deleted: .

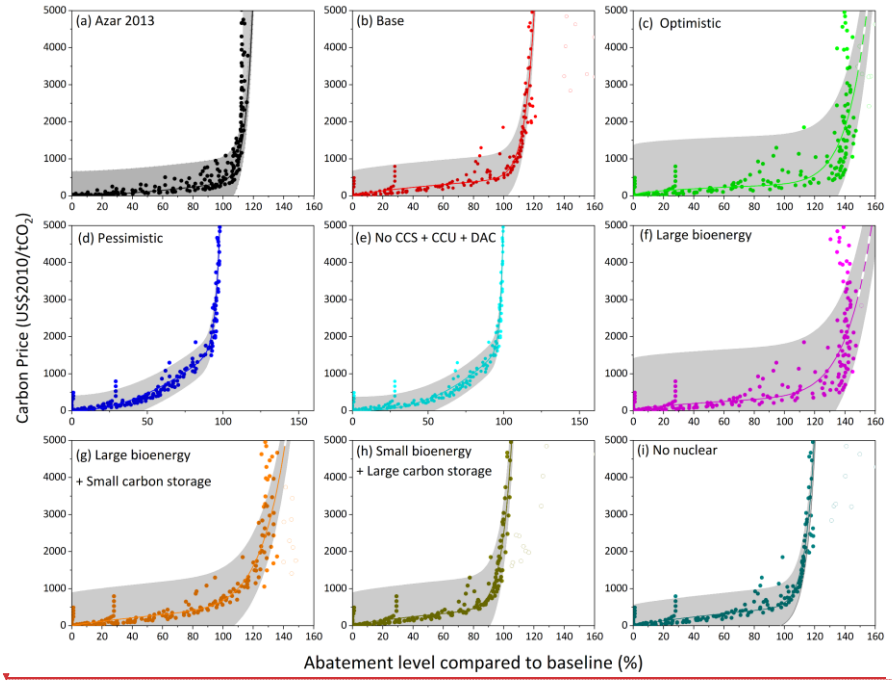

Figure 6. Relationships between the carbon price and the global energy-related CO_2 abatement level obtained from GET with different portfolios of available mitigation technologies. Panel (a) shows the results obtained from an older version of GET (Azar et al., 2013) for the sake of comparison. Panels (b) to (i) show the results from GET (Lehtveer et al., 2019) with different technology portfolios. See Section 2.2 for the definitions of technology portfolios. Points are the data obtained from GET; lines are the MAC curves calculated based on our approach. Open circles are the data that were not considered in the derivation of MAC curves (Table 1) and are typically found after 2100, in some cases above the abatement level of 160% (not shown). Note that we have converted the unit in Panel (a) from US$2010/tC, which is used in the older version of GET, to US$2010/$tCO_2$, the commonly used unit here. The shaded bands are the 95% confidence intervals of the fitted curves calculated (see the caption of Figure 2).

Global MAC curves for energy-related CO_2 emissions from different technology portfolios cover a wide range. The range is almost as wide as that from ENGAGE IAMs (i.e., inter-portfolio range ≈ inter-model range), if we disregard the MAC curve from COFFEE (Figure 2d). The MAC curve from the Base portfolio is generally higher than the MAC curve based on the previous version of the model (Azar et al., 2013; Tanaka and O'Neill, 2018), reflecting the biomass supply potential being smaller in the GET version used in our analysis (i.e., 134 EJ/year) than in the previous version (approximately 200 EJ/year), among other reasons. The maximum abatement level of the Base portfolio is about 120%, which is slightly higher than the estimate of 112% based on the previous model version. The Optimistic portfolio generally gives lower carbon prices and deeper mitigation potentials than the Base portfolio. Conversely, the Pessimistic portfolio shows higher carbon prices and more limited mitigation potential than the Base portfolio. The Optimistic and Large bioenergy portfolios yield more than 150%

Deleted: 6.

Deleted: UD

Deleted: span

Deleted: nearly

Deleted: technology

Deleted: potentials

CO_2 abatement levels at maximum. The Large bioenergy + Low carbon storage portfolio gives lower maximum abatement levels than the previous two portfolios due to the assumed lower carbon storage potential. The Low bioenergy + Large carbon storage portfolio limits the maximum CO_2 abatement levels at only slightly above 100%. With the Pessimistic portfolio, the maximum CO_2 abatement levels do not exceed 100% (i.e., no net negative CO_2 emissions) primarily because no carbon capture technologies such as CCS, CCU, and DAC are available. Likewise, the No CCS+CCU+DAC portfolio also gives a maximum abatement level below 100%. The No nuclear portfolio gives a similar relationship to the one from the Base portfolio, indicating a limited role of nuclear energy here. Finally, the results are somewhat, but not strongly, sensitive to the choice of discount rate (5% by default), as indicated by the results based on alternative discount rates of 3% and 7%, where the growth rate of carbon price is fixed at the value of the respective discount rate based on the Hotelling rule (Figure S89). The deployment of some technologies leads to a rapid increase and then a decrease in the increase rate of abatement price, as reflected in values of b less than 1 and values of d greater than 1 (Table 3). In general, a policy mix with more technologies leads to lower carbon costs, despite the relatively high upfront costs of technology deployment and use.

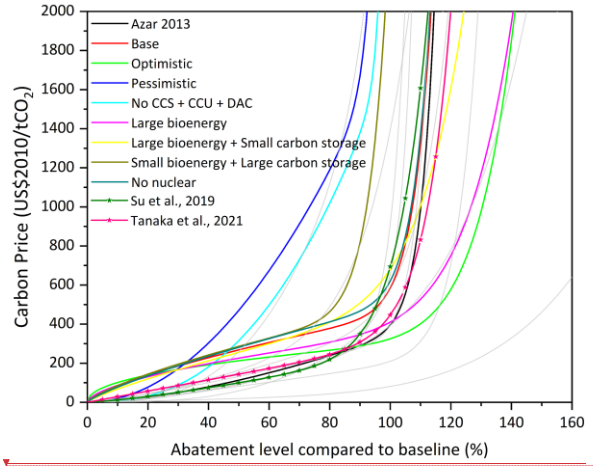

Figure 7. Global MAC curves for energy-related CO_2 emissions derived from the GET model with different portfolios of available mitigation technologies. Different colors indicate different technology portfolios (see Section 2.2 for details). Global MAC curves for energy-related CO_2 emissions from ENGAGE IAMs are shown as a comparison in gray lines, and the MAC curves from selected previous studies (Su et al., 2017; Tanaka et al., 2021) are shown in star-shaped lines.

Technology portfolio	Gas	*a*	*b*	*c*	*d*	MaxABL	Max1st	Max2nd
Azar 2013	CO_2	338.61	1.58	57.08	24.59	112	5.6	0.9
Base	CO_2	441.86	0.72	142.54	18.73	121	7.4	1.3
Optimistic	CO_2	292.67	0.46	32.43	11.41	148	11.5	2.1
Pessimistic	CO_2	1839.19	1.97	6716.35	34.62	100	4.5	0.8
No CCS + CCU + DAC	CO_2	1775.74	2.49	3707.48	53.90	100	5.4	0.9

Deleted: from
Deleted: in which
Deleted:
Moved down [36]: 3707.48
Moved down [38]: 53.90
Moved up [35]: 1775.74
Moved up [37]: 2.49
Moved (insertion) [35]
Moved (insertion) [37]
Moved (insertion) [36]
Moved (insertion) [38]

Large bioenergy	CO_2	340.99	0.59	69.68	9.17	148	11.3	2.0
Large bioenergy + Small carbon storage	CO_2	452.10	0.82	229.12	8.52	140	7.6	1.5
Small bioenergy + Large carbon storage	CO_2	480.65	0.75	1992.76	15.93	105	6.1	1.1
No nuclear	CO_2	489.97	0.80	131.23	19.52	120	7.2	1.3

Table 3. Parameter values of global MAC curves for energy-related CO_2 emissions derived from GET and associated limits on abatement. See equation (1) for parameters *a*, *b*, *c*, and *d*. The units for *a* and *c* are US$2010/t$CO_2$. MaxABL denotes the maximum abatement level (%) of each gas indicated from GET simulation data. Max1st and Max2nd represent the maximum first and second derivatives (%/year and %/(year)^2), respectively, of abatement changes.

4. Validation of ACC2-emIAM

4.1 ACC2 model

To validate the performance of our MAC curves emulating IAM responses (i.e., emIAM), we couple emIAM with the ACC2 model (ACC2-emIAM). ACC2 dates back to the impulse response functions of the global carbon cycle and climate system (Hasselmann et al., 1997; Hooss et al., 2001; Bruckner et al., 2003). The model was later developed to a simple climate model with a full set of climate forcers (Tanaka et al., 2007) and then to the current form (Tanaka et al., 2013; Tanaka and O'Neill, 2018; Tanaka et al., 2021): a simple climate-economy model[1] that consists of i) carbon cycle, ii) atmospheric chemistry, iii) physical climate, and iv) mitigation modules.

The representations of natural Earth system processes in the first three modules of ACC2 are at the global-annual-mean level as in other simple climate models (Joos et al., 2013; Nicholls et al., 2020). The carbon cycle module falls into the category of box models (Mackenzie and Lerman, 2006) and the physical climate module is a heat diffusion model DOECLIM (Kriegler, 2005). ACC2 covers a comprehensive set of direct and indirect climate forcers: CO_2, CH_4, N_2O, O_3, SF_6, 29 species of halocarbons, OH, NO_x, CO, VOC, aerosols (both radiative and cloud interactions), and stratospheric H_2O. The model captures key nonlinearities, for example, those associated with CO_2 fertilization, tropospheric O_3 production from CH_4, and ocean heat diffusion. Uncertain parameters are optimized (Tanaka et al., 2009a, b; Tanaka and Raddatz, 2011) based on an inverse estimation theory (Tarantola, 2005). The equilibrium climate sensitivity is assumed at 3 °C, the best estimate of IPCC (2021). The mitigation module contains a set of global MAC curves for CO_2, CH_4, and N_2O (Johansson, 2011; Azar et al., 2013), which is a previous version of MAC curves to be replaced with the MAC curves derived in this study. ACC2 can be

[1] ACC2-emIAM (and ACC2 with the previous version of MAC curves) can be broadly viewed as an IAM, that is, a simple cost-effective IAM that considers global mitigation costs relative to an assumed baseline. In terms of the level of simplicity, ACC2-emIAM is similar to the DICE model (Nordhaus, 2017) and other simple cost-benefit IAMs that inform the social cost of carbon (Errickson et al., 2021; Rennert et al., 2022). However, ACC2-emIAM does not have an economic growth model and does not account for climate damage. In this study, ACC2-emIAM is characterized as a climate-economy model, but not an IAM, to distinguish it from the more complex IAMs emulated by the MAC curves. ACC2-emIAM also differs from these complex IAMs, which are typically not directly coupled with a climate model, with some versions of GET (Azar et al., 2013; Gaucher et al., 2023) being exceptions.

Moved down [40]: 229.12
Moved up [39]: 452.10
Moved up [41]: 0.82
Moved (insertion) [39]
Moved (insertion) [41]
Moved (insertion) [40]
Deleted: 8.52
Deleted:
Deleted: 3.
Deleted: UD
Deleted: ((%/
Deleted:)
Deleted: (%/
Deleted: tests for
Deleted: -ACC2
Deleted: .
Deleted:
Deleted: IPCC (2021)
Deleted: discussed

used to optimize CO_2, CH_4, and N_2O emission pathways based on a cost-effectiveness approach. That is, the model can calculate least-cost emission pathways for the three gases since year 2020, while meeting a specified climate target (e.g., 2 °C warming target) with the lowest total cumulative mitigation costs in terms of the net present value. The model is written in GAMS and numerically solved using CONOPT3 and CONOPT4, the solvers for nonlinear programming or nonlinear optimization problems available in GAMS.

More specifically, ACC2 uses equation (2) to calculate the abatement costs (ABC) of regions (or global total), gases, and years.

$$ABC_{t,r,g} = Eb_{t,r,g} \cdot \int_0^x f_{t,r,g}(x)dx \quad (2)$$

where t, r, g represent year, region, and gas, respectively. x is the abatement level compared to the baseline scenario. $f_{t,r,g}(x)$ is the MAC function. Eb is the baseline emission level for the IAM. The objective of the model is to minimize the net present value of the total abatement cost ($TABC$), that is:

$$\min TABC = \sum_{t,r,g} \frac{ABC_{t,r,g}}{(1+DSC)^{t-t0}} \quad (3)$$

where DSC is the discount rate and $t0$ represents the base year used for abatement cost calculations (2010 in this study).

In this study, we replace the existing set of MAC curves in ACC2 with the global and regional MAC curves obtained in this study. We also replace the limits on abatement (i.e., upper limits on abatement levels and their first and second derivatives) with those obtained from this study. We assume a 5% discount rate in the validation tests, a rate commonly assumed in IAMs (Emmerling et al., 2019), which is also consistent with some of the IAMs analyzed here such as MESSAGE and GET (Figures SI 1.2-1 and 1.2-2 of Riahi et al. (2021)). But we were unable to find the discount rates used in the other IAMs. Note that a 4% discount rate was used as default in recent studies using ACC2 (Tanaka and O'Neill, 2018; Tanaka et al., 2021). We consider the mitigation costs through 2100 in scenario optimizations.

4.2 Experimental setups for the validation tests

The emission pathways of ENGAGE IAMs were generated under a series of cumulative carbon budgets (or corresponding carbon price pathways) (Section 2.1). Those of GET were calculated under a series of carbon price pathways (Section 2.2). All these pathways are not directly linked to a temperature target, which is typically used as a constraint for ACC2. Therefore, we successively validated the performance of ACC2-emIAM by applying a constraint first on the cumulative emission budget (Test 1) and then on the global-mean temperature (Tests 2 to 4). Four types of experiments were progressively performed as summarized in Table 4. Test 1 mimics the condition under which the ENGAGE IAM simulations were carried out, and can thus be regarded as a direct validation of MAC curves. Tests 2 to 4 are more applied validations to check how MAC curves can work with a simple climate model. Tests 2 to 4 can also be seen as applications, rather than validations, of emIAM for temperature targets because the ACC2-emIAM setup takes into account the individual gas characteristics such as the short lifetime of CH_4 in deriving least-cost emission pathways, which the original IAM setups do not take into account (i.e., using

Deleted: derive

Deleted: variety of

Deleted: from our

Deleted: further

Deleted: . In fact, we were not able to find the estimates of discount rates used in ENGAGE IAMs, but we inferred the discount rate used in MESSAGE by comparing

Deleted: with data in ENGAGE Scenario Explorer. Note that a 4% discount rate was used as default in recent studies using ACC2 (Tanaka and O'Neill, 2018; Tanaka et al., 2021). We discuss the results until 2100 thus consider the mitigation costs until 2100 in scenario optimizations. With the updates described above, we generate cost-effective pathways through emIAM-ACC2

Deleted: emIAM-ACC2 (and ACC2 with the previous version of MAC curves) can be regarded broadly as an IAM, that is, a simple cost-effective IAM considering global mitigation costs relative to an assumed baseline. In terms of the level of simplicity, emIAM-ACC2 is akin to the DICE model (Nordhaus, 2017) and other simple cost-benefit IAMs informing the social cost of carbon (Errickson et al., 2021; Rennert et al., 2022). However, emIAM-ACC2 does not have an economic growth model and does not consider climate damage. In this study, emIAM-ACC2 is characterized as a climate-economy model, but not an IAM, to distinguish itself from the more complex IAMs emulated by the MAC curves. emIAM-ACC2 is also different from these complex IAMs, which are usually not directly coupled with a climate model, with a previous version of GET (Azar et al., 2013) being an exception. ACC2 itself is a hybrid of a simple climate model and a climate-economy model, depending on how the model is used (i.e., with or without the mitigation module). For the sake of discussion, ACC2 is characterized as a simple climate model in this paper when it is coupled with MAC curves obtained from this study.

Deleted: with

Deleted: related

Deleted: Given this

Deleted: -ACC2 successively

Deleted: a

Deleted: for how

Deleted: original

Deleted: . Thus, it

Deleted: test for

Deleted: , strictly speaking.

Deleted: practical test

Deleted: an applied setting. However, the settings of these three tests deviate from how

Deleted: simulations were performed. The outcomes of these three tests are influenced by how the temperature target is set.

GWP100 weighting instead).

	Test 1	Test 2	Test 3	Test 4
Target	Emission budget	2100 temperature	2100 temperature	2100 temperature Peak temperature
Variable	Separately, gas by gas	Separately, gas by gas	Simultaneously all three gases	Simultaneously all three gases

Table 4. Experimental designs of the validation tests for ACC2-emIAM. See text for details.

- Test 1: Constraint on the cumulative emission budget of each gas. We generate least-cost emission pathways with a cap on the cumulative emissions of each gas separately (total anthropogenic CO_2, CH_4, and N_2O emissions for ENGAGE IAMs; energy-related CO_2 emissions for GET). The cap on CO_2 for an ENGAGE IAM is equal to the cumulative carbon budget as specified in each ENGAGE IAM simulation. The cap on CO_2 for GET was calculated from the output of GET, which was simulated under carbon price pathways. The caps on CH_4 and N_2O for ENGAGE IAMs were obtained by calculating the respective cumulative emissions from 2019 to 2100. Note that the cumulative CH_4 budget, or an emission budget of short-lived gases in general, does not offer any useful physical interpretation, while the cumulative CO_2 budget, or an emission budget of long-lived gases, can be an indicator of the global-mean temperature change (Matthews et al., 2009; Allen et al., 2022). It should also be noted that this experiment does not directly make use of the carbon cycle, atmospheric chemistry, and physical climate modules of ACC2 (i.e., simple climate models), as these modules do not affect the results. Test 1 evaluates how the cumulative emission budget can be distributed over time, which depends on the MAC curves and the limits on abatement (i.e., upper limits on abatements and their first and second derivatives), while minimizing the total abatement costs.

- Test 2: Constraint on the end-of-century warming for one gas at a time. We first use ACC2 to calculate the temperature pathway from each carbon budget scenario of each IAM. The calculated temperature at the end of the century is used as a constraint on ACC2-emIAM. This test does not use the temperature data found in the ENGAGE Scenario Explorer, which were calculated using different simple climate models (Xiong et al., 2022). We calculate least-cost emission pathways for only one gas at a time (CO_2, CH_4, or N_2O for ENGAGE IAMs). For example, when calculating a least-cost emission pathway for CO_2, we assume the CH_4 and N_2O emissions to follow the respective pathways from the corresponding carbon budget scenario in the ENGAGE Scenario Explorer. This test validates the temporal distribution of emissions under an end-of-century warming target with global MAC curves. It also validates the trade-off among different regions with regional MAC curves; however, it does not address the trade-off among different gases.

- Test 3: Constraint on the end-of-century warming for three gases simultaneously. This test is the same as Test 2, except that it calculates least-cost emission pathways for three gases simultaneously (CO_2, CH_4, and N_2O for ENGAGE IAMs).

Deleted:
Deleted:
Deleted:
Deleted: 4.
Deleted: -ACC2
Deleted: equivalent
Deleted: model) since
Deleted: influence
Deleted: But this test is about the way
Deleted: with
Deleted: being minimized
Deleted: -the
Deleted: -
Deleted: -
Deleted: -
Deleted: temperature
Deleted: -ACC2. To keep consistency with the emission budget, this
Deleted: for
Deleted: we compute
Deleted: available
Deleted: the-
Deleted: and additionally
Deleted: validate
Deleted: the-
Deleted: are calculated simultaneously

This test validates not only the aspects described for Test 2 but also the trade-off among different gases. Note that we do not use GWP100 in ACC2-emIAM to generate least-cost pathways for CO_2, CH_4, and N_2O. In other words, abatement levels among the three gases are determined directly by the MAC curves without being constrained by GWP100. It is well-known that the use of GWP100 in an IAM leads to a deviation from the cost-effective solution (O'Neill, 2003; Reisinger et al., 2013; Berg et al., 2015; Tanaka et al., 2021). Although the deviation is unlikely to be very large, this can be a small source of discrepancy between the original and reproduced pathways.

- Test 4: Constraint on the end-of-century warming and the mid-century peak warming for three gases simultaneously. This test is the same as Test 3, except that the maximum temperature in mid-century is used as an additional constraint on ACC2-emIAM. The peak temperature was taken from the temperature calculation using ACC2 performed for Test 2. The constraint of the mid-century peak warming is intended to control near-term CH_4 emissions, which are known to have a strong effect on peak temperatures in mid-century but little effect on end-of-century temperatures (Shoemaker et al., 2013; Sun et al., 2021; Xiong et al., 2022; McKeough, 2022).

There are other technical notes that apply to all four tests above. For PKB scenarios, we impose a condition that prohibits net negative CO_2 emissions on ACC2-emIAM. For ECB scenarios (for Test 1 only), we assume that a carbon budget can be interpreted simply as a net budget when it is related to the final temperature through the property of the Transient climate response to cumulative carbon emissions (TCRE), as commonly assumed in the IAM community. It should, however, be noted that such an assumption may not hold for large temperature overshoot scenarios (Tachiiri et al., 2019; Melnikova et al., 2021; Zickfeld et al., 2021; Mastropierro et al., 2023). For scenarios with INDC, which follow NDC up to 2030, we impose the original scenarios up to 2030 and perform the optimization from 2030 onwards. For scenarios without INDC, on the other hand, we perform the optimization starting in 2020. Emissions scenarios for all GHGs and air pollutants other than the three gases are assumed to follow the corresponding scenarios from ENGAGE Scenario Explore or the most proximate SSP in the case of GET. The original scenarios from GET are available from 2010, but we reproduced the GET scenarios from 2020 (as done for ENGAGE IAMs) and adopted the GET scenarios from 2010 to 2020 in ACC2-emIAM. When a scenario was removed from the MAC curve fitting (Table 1), the scenario was also removed from the validation.

It is important to note that the outcome of the tests described above needs to be interpreted differently, depending on whether the IAM is an intertemporal optimization model or a recursive dynamic model (Table 1) (Babiker et al., 2009; Guivarch and Rogelj, 2017; Melnikov et al., 2021). While the temporal distribution of emission abatement is internally calculated in an intertemporal optimization model, it is typically an a priori assumption in a recursive dynamic model and determined by a given carbon price pathway. In a recursive dynamic model, the underlying economic and energy-related relationships that determine the temporal distribution of emission abatement are not necessarily consistent with those used to

Deleted: offs
Deleted: It should be noted
Deleted: -ACC2
Deleted: emissions
Deleted: through
Deleted: a
Deleted: probably not
Deleted: in the scenarios simulated with the IAMs here
Deleted: emission
Deleted: the-
Deleted: -ACC2
Deleted: as done in
Deleted: for each carbon budget scenario of each IAM.
Deleted: aims
Deleted: influence
Deleted: impacts
Deleted: impacts
Deleted: the-
Deleted: There are further technical notes applied to all four tests above. When the scenario allows only a limited or no temperature overshoot (i.e., scenarios without 'f'; see Section 2.1), we impose a condition prohibiting net negative CO_2 emissions on emIAM-ACC2. In Test 1, when the scenario allows a temperature overshoot (i.e., scenarios with 'f'), we assume that a carbon budget can be interpreted simply as a net budget as commonly assumed in the IAM community, although such an assumption may not hold under large temperature overshoot scenarios (Tachiiri et al., 2019; Melnikova et al., 2021; Zickfeld et al., 2021). For INDCi2030 scenarios, which follow NDCs until 2030, we impose the original scenarios until 2030 and perform the optimization from 2030. For NPi2020 scenarios, on the other hand, we perform the optimization from 2020. For emissions scenarios of all GHGs and air pollutants other than the three gases, we prescribe corresponding scenarios from ENGAGE Scenario Explore or the most proximate SSP in the case of GET.
Deleted: usually
Deleted: either by a given emission pathway or
Deleted: may
Deleted: be

allocate emission abatement across sectors and regions at each time step.

4.3 Results from the validation tests

Figure 8 provides an overview of the validation results, using REMIND as an example. Overall, ACC2-emIAM has closely reproduced the original CO_2 emission pathways from REMIND in the series of four tests. The outcomes for CH_4 and N_2O were also generally satisfactory, although not as successful as those for CO_2. For Test 1, the results were good for all three gases. The results were similarly good for Test 2, except for a minor discrepancy due to a small rise in emissions at the end of the century. A small increase in emission is known to occur in ACC2 before a temperature target is reached after an overshoot due to the inertia of the system (Tanaka et al., 2021). However, discrepancies were found in Test 3 for the near-term CH_4 pathways in low budget cases and the late-century CH_4 and N_2O pathways in high budget cases. The discrepancy for near-term CH_4 emissions was reduced in Test 4. CH_4 abatements tend to be incentivized later in the century in the cost optimization of ACC2 with the discount rate of 5% (Tanaka et al., 2021). This effect can be offset by the additional constraint on the mid-century peak temperature, as near-term CH_4 emissions can strongly influence mid-century temperatures (Shoemaker et al., 2013; Sun et al., 2021; Xiong et al., 2022; McKeough, 2022). When interpreting the validation tests, it is useful to keep in mind that only Test 1 can be strictly considered as a pure validation; certain levels of discrepancies can be expected from Tests 2 to 4 due to the difference in the model setup between the original IAMs and ACC2-emIAM.

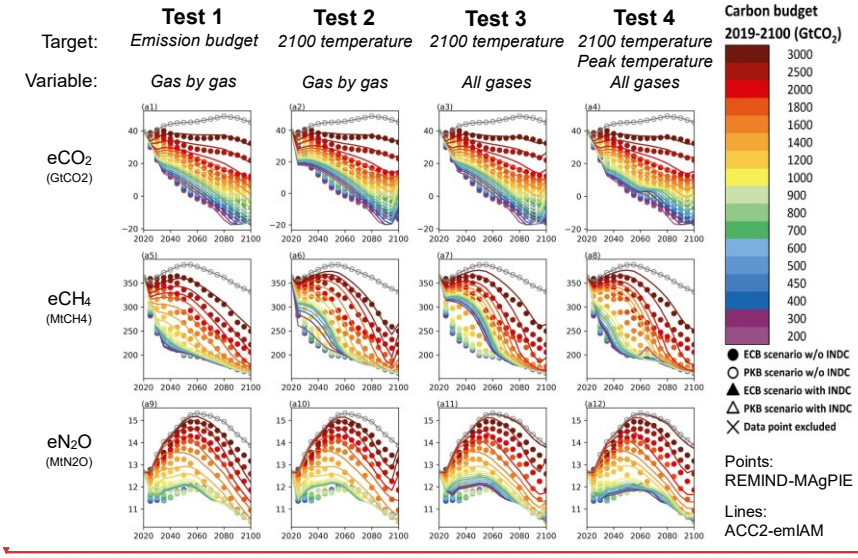

Deleted: -ACC2

Deleted: also

Deleted: if

Deleted: in general. When the test was performed for each gas with the emission budget (

Deleted:),

Deleted: similar with the 2100 temperature target for each gas (…

Deleted:),

Deleted: arising from

Deleted: rise

Deleted: achieved

Deleted: when such a test was performed simultaneously for three gases (Test 3), the results indicated

Deleted: from

Deleted: carbon

Deleted: from

Deleted: carbon

Deleted: of

Deleted: seemed to have been caused by the trade-off between CH_4 and N_2O: the N_2O MAC curve underestimates the prices at high abatement levels (above 20% for N_2O) (Figure S20), which might have led to an overestimate of N_2O abatements and, in turn, an underestimate of CH_4 abatements. The discrepancy for near-term CH_4 emissions was narrowed down with the additional constraint on peak temperatures in mid-century (

Deleted:).

Deleted: high

Deleted: compensated

Deleted: in mid-century because

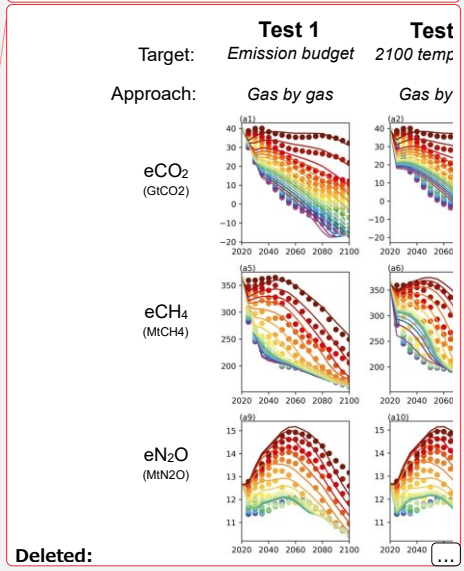

Deleted: …

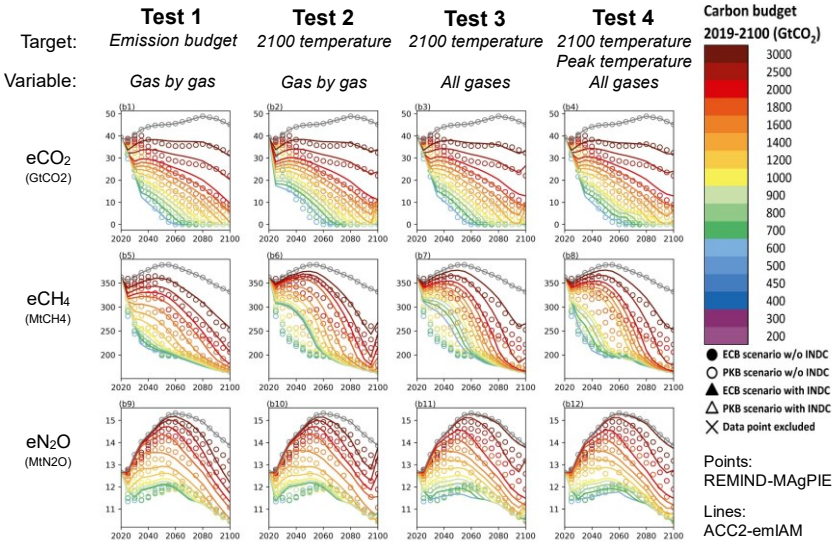

Figure 8. Overview of the validation results for ACC2-emIAM with REMIND as an example. The outcomes for ECB scenarios (filled circles) are shown in the upper set of panels; those for PKB scenarios (open circles) are in the lower set of panels. The points show the original emission pathways from REMIND obtained from the ENGAGE Scenario Explorer; the lines show the emission pathways reproduced from ACC2-emIAM. The same color is used for each pair of original and reproduced pathways. For the sake of presentation, only the outcomes of scenarios without INDC are presented; the outcomes of scenarios with INDC are not shown here. The outcomes of the full set of scenarios can be seen in Figure S90.

Figure 9 shows the validation results from Test 4 for all nine ENGAGE IAMs (global total anthropogenic CO_2, CH_4, and N_2O emissions) and GET with different technology portfolios (global energy-related CO_2 emissions). The full validation results from Tests 1 to 4 can be found in Figures S91-S109, S129-S147, S167-S184, and S203-S220, respectively. CO_2 emission pathways were generally well reproduced through ACC2-emIAM for all ENGAGE IAMs. The outcomes for CH_4 and N_2O were not as good as those for CO_2: only a subset of ENGAGE IAMs such as REMIND and WITCH was adequately captured by ACC2-emIAM. Some of the mismatches can be explained, for example, by the poor fits of N_2O MAC curves from COFFEE and TIAM (Figure S10). The general difficulty in capturing IMAGE through MAC curves (Figure S16) can be seen in the mismatches in these tests for IMAGE in Figure 9. It is also worth noting that, despite very good fits of MAC curves from GEM (Figure S15), CH_4 and N_2O emission pathways were not well reproduced. The results for GET were also generally good, but the Large bioenergy + Small carbon storage portfolio gave a relatively poor result. This may be due to the relatively poor fit of the MAC curve for this technology portfolio, compared to those from other portfolios (Figure 6).

Deleted: 8.
Deleted: -ACC2
Deleted: scenarios with "f" (i.e., net-negative emissions
Deleted:))
Deleted: scenarios without "f" (i.e., net-zero CO_2 emissions…
Deleted:))
Deleted: -ACC2
Deleted: Scenario names indicate respective cumulative carbon budgets for the period 2019 – 2100 in $GtCO_2$. NPi2100 is the baseline scenario for our analysis (black open circles).
Deleted: NPi2020
Deleted: , which consider currently implemented national policies,
Deleted: INDCi2030
Deleted: , which further consider national emission pledges until 2030,
Deleted: ,
Deleted: entire
Deleted: S90-S108, Figures S128-S146, Figures S166-S183…
Deleted: Figures S202-S216
Deleted: -ACC2
Deleted: reasonably well
Deleted: -ACC2
Deleted: S11
Deleted: S17
Deleted: mentioning
Deleted: in spite of
Deleted: of
Deleted: S16
Deleted: of GEM
Deleted: might have been caused by

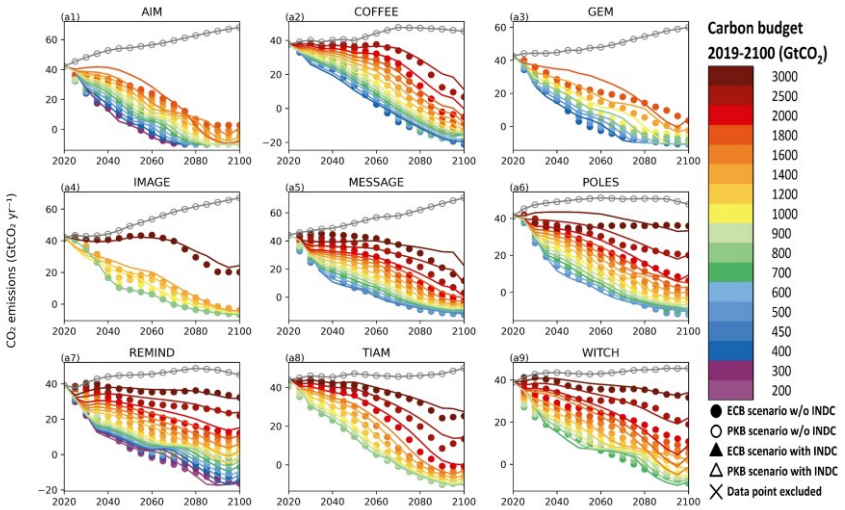
(a1) AIM
(a2) COFFEE
(a3) GEM
(a4) IMAGE
(a5) MESSAGE
(a6) POLES
(a7) REMIND
(a8) TIAM
(a9) WITCH
CO₂ emissions (GtCO₂ yr⁻¹)
Carbon budget
2019-2100 (GtCO2)
3000
2500
2000
1800
1600
1400
1200
1000
900
800
700
600
500
450
400
300
200
ECB scenario w/o INDC
PKB scenario w/o INDC
ECB scenario with INDC
PKB scenario with INDC
Data point excluded

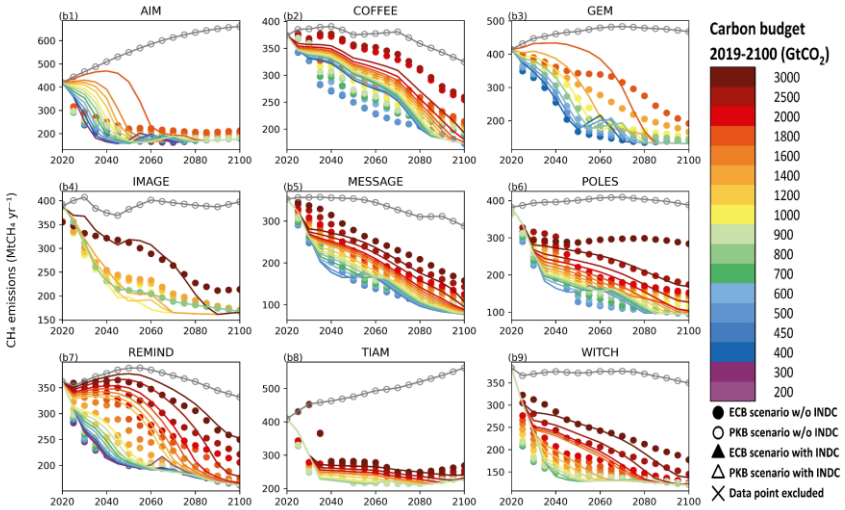
(b1) AIM
(b2) COFFEE
(b3) GEM
(b4) IMAGE
(b5) MESSAGE
(b6) POLES
(b7) REMIND
(b8) TIAM
(b9) WITCH
CH₄ emissions (MtCH₄ yr⁻¹)
Carbon budget
2019-2100 (GtCO2)
3000
2500
2000
1800
1600
1400
1200
1000
900
800
700
600
500
450
400
300
200
ECB scenario w/o INDC
PKB scenario w/o INDC
ECB scenario with INDC
PKB scenario with INDC
Data point excluded

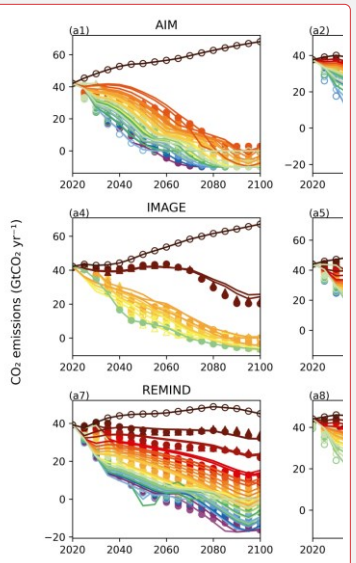
(a1) AIM
(a4) IMAGE
(a7) REMIND
CO₂ emissions (GtCO₂ yr⁻¹)

Deleted:

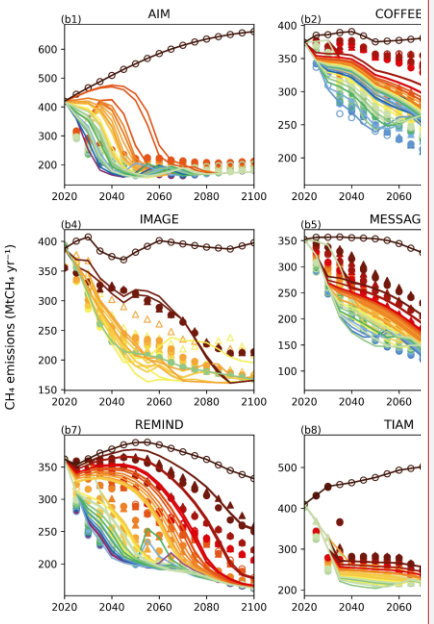
(b1) AIM
(b2) COFFEE
(b4) IMAGE
(b5) MESSAG
(b7) REMIND
(b8) TIAM
CH₄ emissions (MtCH₄ yr⁻¹)

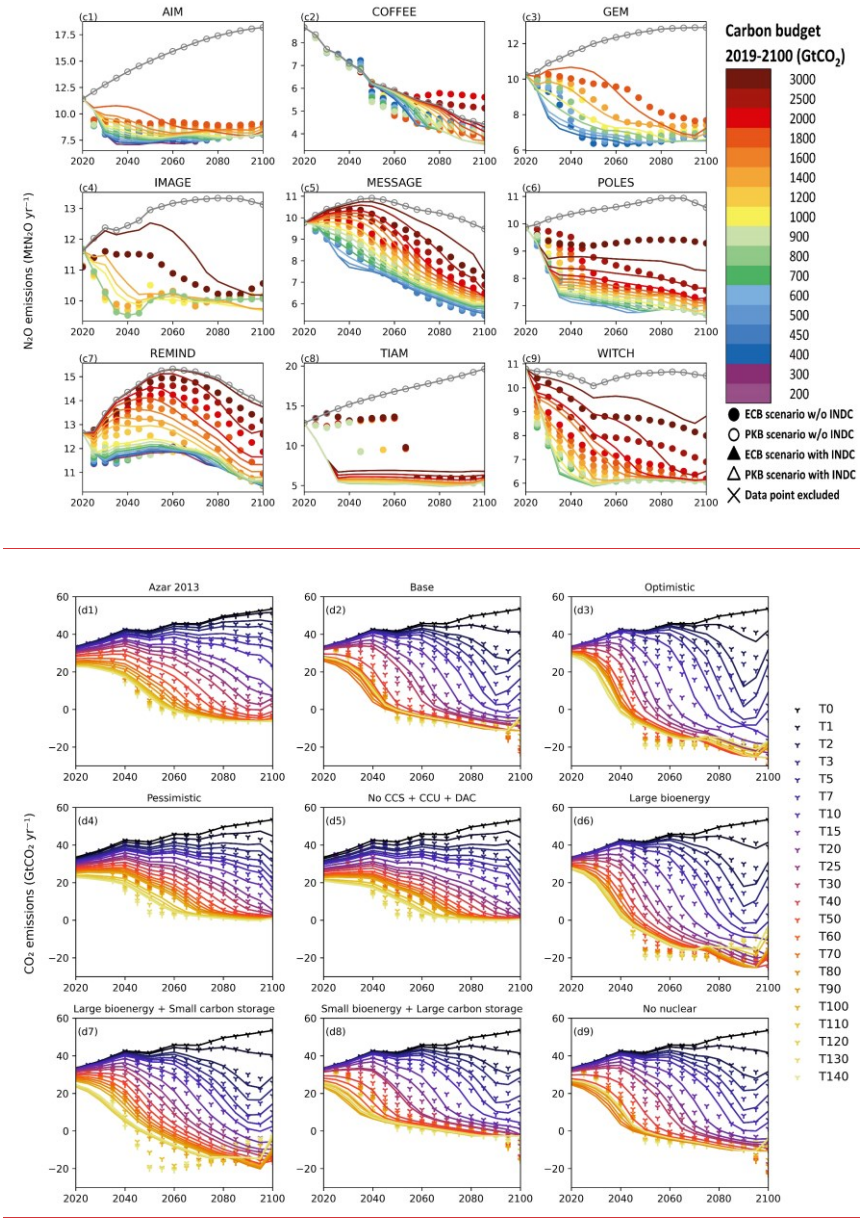

Figure 9. Original and reproduced global emission pathways from Test 4 for nine ENGAGE IAMs (total anthropogenic CO_2, CH_4, and N_2O emissions) and GET (energy-related CO_2 emissions) with different technology portfolios. The first three sets of panels are from the nine ENGAGE IAMs. For the sake of presentation, only the outcomes of ECB scenarios without INDC are presented; those of the full scenarios can be seen in Figures S203 to S205. The last set of panels is from GET with different technology portfolios. The points show the original emission pathways from ENGAGE IAMs and GET; the lines show the emission pathways reproduced from

Deleted: 9.

ACC2-emIAM. The same color is used for each pair of original and reproduced pathways. For the legend of the panels for GET, the number indicates the initial carbon price (US$2010/tCO$_2$), from which the carbon price grows 5% each year.

Deleted: -ACC2

Deleted: ENGAGE IAMs, see the caption of Figure 8. For the legend of the panel for

Furthermore, we examine several selected features of the original and reproduced emission pathways from Test 4 (ECB scenarios without INDC only), such as CO_2 emissions in 2030, 2050, and 2100, cumulative negative CO_2 emissions from 2020 to 2100, the year to net zero for CO_2, and that for GHG. Figure 10a-c indicates that the reproducibility of CO_2 emissions for three different points in time varies across models and carbon budgets, but it is worth noting that ACC2-emIAM nearly consistently overestimates and underestimates 2030 CO_2 emissions from AIM and REMIND, respectively. Cumulative negative CO_2 emissions are negatively underestimated for COFFEE (Figure 10d), which is related to the general overestimation of 2100 CO_2 emissions for COFFEE (Figure 10c). The year to net zero for CO_2 tends to be overestimated (later than the original year) for REMIND with the carbon budget at or below 800 GtCO$_2$.

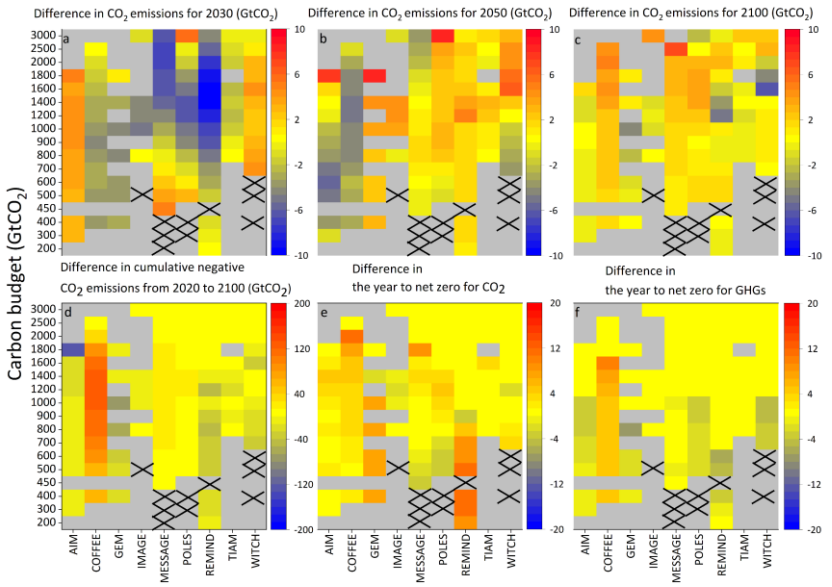

Figure 10. Differences in the pathway features between ENGAGE IAMs and ACC2-emIAM. This figure presents the results from Test 4 for ECB scenarios without INDC. Panels a to c show the difference in CO_2 emissions for 2030, 2050, and 2100, respectively, between ENGAGE IAMs and ACC2-emIAM. Panel d shows the difference in cumulative negative CO_2 emissions. Panels e and f show the difference in the year to net zero for CO_2 and GHG (for CO_2, CH_4, and N_2O), respectively. Positive values indicate that ACC2-emIAM overestimates the pathway feature (i.e., the emulator gives larger emissions (panels a to c), less negative cumulative emissions (panel d), or later year (panels e and f), while negative values indicate the opposite. Gray boxes without black crosses indicate that the corresponding scenarios were not available in the ENGAGE Scenario Explorer, while those with black crosses indicate that the

corresponding scenarios were available but not successfully reproduced by ACC2-emIAM (i.e., infeasible solutions).

4.4 Statistics of the validation tests

To measure to what extent emission pathways obtained from ACC2-emIAM, denoted as y, agree with original pathways from ENGAGE IAMs and GET, denoted as x, we calculate the following two different indicators: i) ordinary Pearson's correlation coefficient r_P and ii) Lin's concordance coefficient r_C. Each of these indicators is discussed below.

First, because of the prevalent use of r_P and its square form (i.e., coefficient of simple determination, so-called r^2) in numerous applications, we use r_P as a reference for comparison, although r_P is known to be inappropriate for testing agreement: it is suited to test the strength of linear relationship, but not the strength of agreement (Bland and Altman, 1986; Cox, 2006). More specifically, r_P (and r^2) shows the strength of linear regression line $\acute{y} = \alpha\acute{x} + \beta$, not necessarily $\acute{y} = \acute{x}$, a special case of agreement. Note that it is possible to calculate r^2 based on $\acute{y} = \acute{x}$ by using the sum of square of residuals and the total sum of squares (i.e., not equation (2)); however, if $\acute{y} = \acute{x}$ is a very poor regression line, r^2 can become negative (page 21 of Hayashi (2000)) and cannot be interpreted as a square of r_P. Other arguments that suggest a more restricted use of r_P can be found elsewhere (Ricker, 1973; Laws, 1997; Tanaka and Mackenzie, 2005). For our application, r_P is defined as below.

$$r_P = \frac{\sum_{i=1}^{l}\sum_{j=1}^{m}(x_{i,j}-\bar{x})(y_{i,j}-\bar{y})}{\sqrt{\sum_{i=1}^{l}\sum_{j=1}^{m}(x_{i,j}-\bar{x})^2}\sqrt{\sum_{i=1}^{l}\sum_{j=1}^{m}(y_{i,j}-\bar{y})^2}} \quad (4)$$

where $x_{i,j}$ and $y_{i,j}$ are the original and reproduced emission, respectively, for year i (for $i = 1, \dots, l$) under scenario j (for $j = 1, \dots, m$). $\bar{x}$ and $\bar{y}$ are the mean of $x_{i,j}$ and $y_{i,j}$, respectively, over i and j. r_P can change between -1 and 1. When it is 1, the samples have a perfect linear relationship, which is a necessary condition for a perfect agreement. When it is 0, there is no linear relationship in the samples.

Second, r_C is a more appropriate indicator for measuring agreement than r_P (Lin, 1989; Barnhart et al., 2007; Lin et al., 2012). r_C is defined as follows.

$$r_C = \frac{2s_{xy}}{s_x^2+s_y^2+(\bar{x}-\bar{y})^2} \quad (5)$$

where s_x^2 and s_y^2 are the variance of $x_{i,j}$ and $y_{i,j}$, respectively. That is, $s_x^2 = \frac{1}{l\times m}\sum_{i=1}^{l}\sum_{j=1}^{m}\left(x_{i,j}-\bar{x}\right)^2$ and $s_y^2 = \frac{1}{l\times m}\sum_{i=1}^{l}\sum_{j=1}^{m}\left(y_{i,j}-\bar{y}\right)^2$, respectively. s_{xy} is the covariance of $x_{i,j}$ and $y_{i,j}$. That is, $s_{xy} = \frac{1}{l\times m}\sum_{i=1}^{l}\sum_{j=1}^{m}\left(x_{i,j}-\bar{x}\right)\left(y_{i,j}-\bar{y}\right)$. r_C also distributes between -1 and 1. When it is 1, 0, and -1, it indicates a perfect concordance, no concordance, and a perfect discordance (or reverse concordance), respectively. r_C is commonly interpreted either similar to r_P or in the following way: >0.99, almost perfect; 0.95 to 0.99, substantial; 0.90 to 0.95, moderate; <0.90, poor (Akoglu, 2018). An underlying assumption for this parametric statistic is that the population follows Gaussian distributions.

Deleted: -ACC2

Deleted: for samples

Deleted: (Martin Bland and Altman, 1986; Cox, 2006).

Deleted: $r_P = \frac{\sum_{i=1}^{l}\sum_{j=1}^{m}(x_{i,j}-\bar{x})(y_{i,j}-\bar{y})}{\sqrt{\sum_{i=1}^{l}\sum_{j=1}^{m}(x_{i,j}-\bar{x})^2}\sqrt{\sum_{i=1}^{l}\sum_{j=1}^{m}(y_{i,j}-\bar{y})^2}}$ (2)

Deleted:

Deleted: $r_C = \frac{2s_{xy}}{s_x^2+s_y^2+(\bar{x}-\bar{y})^2}$ (3)

			AIM	COFFEE	GEM	IMAGE	MESSAGE	POLES	REMIND	TIAM	WITCH
r_P	Test 1	CO_2	0.986	0.990	0.983	0.975	0.981	0.960	0.976	0.985	0.937
		CH_4	0.962	0.977	0.964	0.973	0.975	0.967	0.986	0.927	0.985
		N_2O	0.921	0.966	0.948	0.875	0.985	0.964	0.962	0.466	0.975
	Test 2	CO_2	0.984	0.994	0.982	0.979	0.984	0.987	0.962	0.997	0.973
		CH_4	0.667	0.941	0.805	0.890	0.960	0.954	0.941	0.951	0.962
		N_2O	0.908	0.970	0.777	0.875	0.983	0.969	0.962	0.531	0.981
	Test 3	CO_2	0.983	0.991	0.981	0.974	0.974	0.986	0.975	0.879	0.973
		CH_4	0.678	0.911	0.852	0.886	0.968	0.929	0.907	0.740	0.933
		N_2O	0.933	0.956	0.966	0.600	0.977	0.961	0.948	0.549	0.956
	Test 4	CO_2	0.989	0.990	0.985	0.990	0.981	0.990	0.981	0.995	0.953
		CH_4	0.879	0.916	0.951	0.954	0.978	0.951	0.955	0.953	0.940
		N_2O	0.954	0.955	0.964	0.713	0.977	0.957	0.960	0.607	0.935
r_C	Test 1	CO_2	0.981	0.985	0.981	0.974	0.980	0.955	0.975	0.983	0.918
		CH_4	0.957	0.977	0.960	0.968	0.974	0.966	0.986	0.927	0.984
		N_2O	0.916	0.964	0.946	0.863	0.981	0.963	0.962	0.385	0.972
	Test 2	CO_2	0.979	0.991	0.980	0.978	0.982	0.986	0.962	0.997	0.968
		CH_4	0.549	0.926	0.730	0.833	0.956	0.942	0.919	0.949	0.953
		N_2O	0.901	0.968	0.764	0.863	0.981	0.969	0.961	0.454	0.980
	Test 3	CO_2	0.976	0.988	0.978	0.973	0.971	0.983	0.975	0.877	0.964
		CH_4	0.558	0.905	0.815	0.858	0.962	0.924	0.881	0.715	0.918
		N_2O	0.914	0.954	0.961	0.572	0.975	0.947	0.946	0.494	0.945
	Test 4	CO_2	0.987	0.987	0.982	0.990	0.978	0.987	0.981	0.993	0.949
		CH_4	0.852	0.911	0.934	0.931	0.964	0.933	0.944	0.946	0.935
		N_2O	0.935	0.954	0.956	0.699	0.972	0.940	0.960	0.482	0.920

	GET technology portfolio	Azar2013	Base	Optimistic	Pessimistic	No_cap	L_bio	L_bio/S_str	S_bio/L_str	No_nc
r_P	Test 1	0.992	0.983	0.973	0.991	0.981	0.964	0.964	0.984	0.984
	Test 2	0.985	0.978	0.976	0.982	0.968	0.966	0.964	0.968	0.978
	Test 4	0.985	0.979	0.976	0.981	0.967	0.977	0.973	0.969	0.978
r_C	Test 1	0.992	0.983	0.972	0.991	0.979	0.963	0.964	0.983	0.984
	Test 2	0.985	0.978	0.975	0.981	0.963	0.966	0.964	0.966	0.977
	Test 4	0.985	0.979	0.976	0.980	0.963	0.977	0.973	0.966	0.978

Table 5. Statistical validation of global emission pathways reproduced from ACC2-emIAM with original emission pathways from nine ENGAGE IAMs and GET. The upper and lower panels are the results for ENGAGE IAMs (global total anthropogenic CO_2, CH_4, and N_2O emissions) and GET (global energy-related CO_2 emissions), respectively. The table shows two indicators: i) ordinary Pearson's correlation coefficient r_P and ii) Lin's concordance coefficient r_C. The higher the value of the indicator is, the darker the color of the cell is. See text for the details of these statistical indicators. This table presents the results from all scenarios. Results only from the ECB scenarios without INDC can be found in Table S5.

Deleted:

			AIM	COFFEE
r_P	Test 1	CO_2	0.986	0.990
		CH_4	0.962	0.977
		N_2O	0.921	0.966
	Test 2	CO_2	0.984	0.994
		CH_4	0.667	0.934
		N_2O	0.908	0.962
	Test 3	CO_2	0.983	0.989
		CH_4	0.678	0.914
		N_2O	0.933	0.950
	Test 4	CO_2	0.989	0.990
		CH_4	0.879	0.916
		N_2O	0.954	0.955
r_C	Test 1	CO_2	0.981	0.985
		CH_4	0.957	0.977
		N_2O	0.916	0.964
	Test 2	CO_2	0.979	0.991
		CH_4	0.549	0.926
		N_2O	0.901	0.959
	Test 3	CO_2	0.976	0.986
		CH_4	0.558	0.908
		N_2O	0.914	0.947
	Test 4	CO_2	0.987	0.987
		CH_4	0.852	0.911
		N_2O	0.935	0.954

	GET technology portfolio	Azar2013	Base	Optimistic	Pes
r_P	Test 1	0.992	0.983	0.973	
	Test 2	0.985	0.943	0.973	
	Test 4	0.988	0.945	0.979	
r_C	Test 1	0.992	0.983	0.972	
	Test 2	0.985	0.938	0.973	
	Test 4	0.988	0.940	0.979	

Deleted: 5.

Deleted: -ACC2

Deleted: figure

		Test 1					Test 2					Test 3					Test 4				
		AIM	COFFEE	GEM	IMAGE	MESSAGE	AIM	COFFEE	GEM	IMAGE	MESSAGE	AIM	COFFEE	GEM	IMAGE	MESSAGE	AIM	COFFEE	GEM	IMAGE	MESSAGE
	SUBSAFR	0.954	0.916	0.978	0.963	0.979	0.951	0.938	0.976	0.966	0.978	0.954	0.920	0.971	0.956	0.980	0.961	0.923	0.982	0.978	0.980
	CHN	0.974	0.978	0.978	0.966	0.990	0.970	0.985	0.976	0.965	0.983	0.975	0.982	0.969	0.957	0.986	0.982	0.983	0.980	0.984	0.989
	EUWE	0.979	0.849	0.974	0.973	0.994	0.977	0.869	0.974	0.979	0.982	0.984	0.865	0.975	0.974	0.988	0.982	0.865	0.973	0.988	0.990
	SOUASIA	0.965	0.848	0.964	0.957	0.958	0.961	0.893	0.960	0.956	0.954	0.964	0.890	0.956	0.957	0.956	0.976	0.886	0.968	0.971	0.965
	LATAME	0.964	0.935	0.962	0.909	0.964	0.962	0.947	0.958	0.906	0.959	0.968	0.944	0.952	0.904	0.960	0.964	0.944	0.966	0.920	0.962
CO_2	MIDEAST	0.983	0.870	0.964	0.952	0.979	0.982	0.909	0.953	0.957	0.964	0.985	0.904	0.941	0.952	0.964	0.987	0.903	0.957	0.976	0.961
	NORAM	0.981	0.930	0.959	0.963	0.990	0.980	0.947	0.963	0.965	0.981	0.986	0.940	0.958	0.958	0.987	0.981	0.939	0.961	0.977	0.985
	PACOECD	0.969	0.956	0.966	0.945	0.993	0.967	0.967	0.970	0.944	0.986	0.973	0.964	0.964	0.937	0.990	0.976	0.964	0.968	0.954	0.992
	REFECO	0.986	0.939	0.944	0.969	0.993	0.985	0.951	0.946	0.971	0.985	0.987	0.946	0.943	0.974	0.987	0.988	0.946	0.950	0.982	0.991
	OTASIAN	0.979	0.952	0.970	0.957	0.988	0.977	0.969	0.966	0.957	0.978	0.983	0.963	0.959	0.947	0.982	0.983	0.964	0.972	0.972	0.983
	ROW	0.772	0.881	0.922	0.873	0.659	0.767	0.873	0.875	0.883	0.000	0.790	0.886	0.882	0.870	0.000	0.802	0.887	0.935	0.888	0.000
	SUBSAFR	0.952	0.890	0.949	0.838	0.956	0.556	0.716	0.680	0.691	0.763	0.567	0.699	0.786	0.669	0.800	0.878	0.751	0.931	0.750	0.892
	CHN	0.980	0.988	0.962	0.984	0.980	0.792	0.970	0.783	0.921	0.973	0.800	0.969	0.858	0.942	0.982	0.932	0.975	0.958	0.972	0.989
	EUWE	0.935	0.989	0.920	0.923	0.940	0.695	0.973	0.758	0.770	0.927	0.693	0.970	0.794	0.828	0.927	0.884	0.974	0.879	0.927	0.930
	SOUASIA	0.906	0.533	0.947	0.938	0.930	0.566	0.407	0.717	0.782	0.780	0.567	0.420	0.810	0.829	0.832	0.810	0.497	0.947	0.901	0.903
	LATAME	0.969	0.975	0.962	0.900	0.981	0.752	0.952	0.739	0.811	0.925	0.760	0.967	0.838	0.813	0.953	0.913	0.976	0.962	0.846	0.976
r_P CH_4	MIDEAST	0.966	0.953	0.958	0.801	0.877	0.689	0.906	0.785	0.718	0.817	0.697	0.904	0.857	0.721	0.821	0.897	0.919	0.962	0.832	0.859
	NORAM	0.924	0.942	0.952	0.933	0.979	0.634	0.883	0.698	0.750	0.971	0.630	0.911	0.808	0.797	0.969	0.864	0.922	0.952	0.906	0.975
	PACOECD	0.905	0.909	0.849	0.882	0.958	0.547	0.781	0.471	0.766	0.897	0.544	0.790	0.574	0.784	0.932	0.818	0.811	0.825	0.857	0.958
	REFECO	0.957	0.801	0.968	0.939	0.968	0.737	0.595	0.823	0.749	0.826	0.736	0.637	0.883	0.787	0.881	0.906	0.690	0.967	0.861	0.944
	OTASIAN	0.964	0.970	0.953	0.973	0.994	0.695	0.932	0.807	0.905	0.950	0.701	0.936	0.861	0.931	0.969	0.895	0.949	0.953	0.972	0.986
	ROW	0.895	0.000	0.945	0.000	0.000	0.665	0.000	0.776	0.000	0.000	0.672	0.000	0.836	0.000	0.000	0.782	0.000	0.947	0.000	0.000
	SUBSAFR	0.969	0.953	0.867	0.859	0.902	0.965	0.961	0.885	0.857	0.900	0.979	0.949	0.905	0.776	0.826	0.982	0.950	0.897	0.803	0.837
	CHN	0.982	0.933	0.967	0.971	0.952	0.977	0.934	0.967	0.970	0.945	0.984	0.945	0.980	0.977	0.933	0.982	0.942	0.983	0.983	0.931
	EUWE	0.924	0.967	0.828	0.851	0.971	0.908	0.965	0.805	0.839	0.970	0.951	0.971	0.810	0.703	0.970	0.958	0.971	0.795	0.767	0.974
	SOUASIA	0.913	0.603	0.947	0.863	0.930	0.900	0.801	0.946	0.860	0.933	0.948	0.761	0.966	0.841	0.899	0.939	0.756	0.977	0.843	0.920
	LATAME	0.951	0.807	0.953	0.068	0.930	0.940	0.810	0.954	0.090	0.920	0.968	0.801	0.969	-0.153	0.906	0.957	0.801	0.973	-0.122	0.899
N_2O	MIDEAST	0.874	0.735	0.963	0.984	0.935	0.859	0.742	0.963	0.983	0.936	0.929	0.684	0.971	0.990	0.946	0.922	0.691	0.968	0.992	0.954
	NORAM	0.915	0.899	0.874	0.864	0.930	0.898	0.899	0.899	0.863	0.933	0.948	0.921	0.925	0.807	0.946	0.948	0.919	0.924	0.843	0.947
	PACOECD	0.848	0.811	0.873	0.038	0.971	0.811	0.808	0.906	0.013	0.963	0.916	0.735	0.913	-0.106	0.954	0.925	0.729	0.917	-0.023	0.950
	REFECO	0.926	0.631	0.389	0.430	0.774	0.910	0.630	0.452	0.431	0.780	0.956	0.521	0.518	0.207	0.852	0.956	0.522	0.531	0.263	0.830
	OTASIAN	0.925	0.725	0.933	0.739	0.953	0.908	0.722	0.935	0.737	0.953	0.955	0.673	0.949	0.532	0.962	0.952	0.676	0.939	0.571	0.966
	ROW	0.000	0.000	0.862	0.000	0.998	0.000	0.000	0.879	0.000	0.000	0.000	0.000	0.895	0.000	0.000	0.000	0.000	0.920	0.000	0.000
	SUBSAFR	0.945	0.913	0.976	0.959	0.978	0.941	0.936	0.972	0.980	0.971	0.949	0.913	0.962	0.953	0.977	0.958	0.915	0.972	0.978	0.974
	CHN	0.963	0.972	0.976	0.964	0.989	0.957	0.980	0.972	0.978	0.983	0.968	0.972	0.958	0.954	0.983	0.976	0.973	0.972	0.980	0.986
	EUWE	0.973	0.827	0.941	0.973	0.994	0.971	0.851	0.939	0.982	0.980	0.981	0.828	0.955	0.972	0.986	0.982	0.828	0.951	0.986	0.987
	SOUASIA	0.958	0.737	0.957	0.957	0.952	0.953	0.765	0.953	0.986	0.936	0.959	0.774	0.941	0.956	0.950	0.972	0.769	0.951	0.971	0.956
	LATAME	0.958	0.902	0.951	0.898	0.952	0.956	0.914	0.945	0.962	0.953	0.964	0.908	0.933	0.891	0.940	0.963	0.907	0.949	0.912	0.945
CO_2	MIDEAST	0.978	0.812	0.961	0.951	0.974	0.977	0.845	0.948	0.997	0.949	0.983	0.847	0.924	0.951	0.962	0.986	0.845	0.939	0.974	0.954
	NORAM	0.976	0.909	0.957	0.962	0.985	0.974	0.928	0.961	0.968	0.971	0.983	0.917	0.952	0.956	0.985	0.981	0.914	0.953	0.976	0.979
	PACOECD	0.962	0.940	0.958	0.943	0.993	0.959	0.951	0.963	0.941	0.985	0.968	0.942	0.957	0.935	0.988	0.975	0.941	0.964	0.952	0.988
	REFECO	0.982	0.905	0.940	0.961	0.993	0.980	0.916	0.941	0.957	0.983	0.985	0.908	0.932	0.965	0.986	0.987	0.907	0.941	0.978	0.989
	OTASIAN	0.975	0.935	0.968	0.953	0.987	0.972	0.952	0.965	0.971	0.977	0.982	0.939	0.954	0.941	0.978	0.983	0.939	0.968	0.968	0.977
	ROW	0.705	0.534	0.891	0.561	0.300	0.699	0.518	0.863	0.953	0.000	0.746	0.557	0.866	0.580	0.000	0.751	0.554	0.931	0.591	0.000
	SUBSAFR	0.944	0.885	0.942	0.793	0.953	0.512	0.681	0.537	0.621	0.653	0.514	0.692	0.727	0.628	0.761	0.876	0.745	0.921	0.625	0.861
	CHN	0.973	0.986	0.955	0.978	0.980	0.681	0.962	0.666	0.846	0.962	0.684	0.965	0.810	0.898	0.981	0.912	0.971	0.943	0.957	0.983
	EUWE	0.913	0.989	0.824	0.914	0.932	0.552	0.958	0.757	0.686	0.924	0.536	0.959	0.761	0.784	0.919	0.842	0.967	0.740	0.903	0.914
	SOUASIA	0.894	0.351	0.938	0.927	0.910	0.428	0.239	0.595	0.682	0.662	0.424	0.262	0.755	0.783	0.760	0.772	0.315	0.929	0.848	0.862
	LATAME	0.961	0.972	0.955	0.877	0.981	0.630	0.934	0.614	0.724	0.886	0.629	0.954	0.783	0.757	0.941	0.889	0.966	0.948	0.787	0.973
r_C CH_4	MIDEAST	0.960	0.950	0.953	0.766	0.857	0.566	0.897	0.693	0.638	0.750	0.570	0.902	0.821	0.656	0.762	0.872	0.917	0.952	0.774	0.819
	NORAM	0.903	0.934	0.949	0.919	0.969	0.492	0.792	0.588	0.678	0.971	0.474	0.887	0.766	0.759	0.960	0.821	0.905	0.941	0.850	0.958
	PACOECD	0.888	0.907	0.841	0.841	0.957	0.409	0.709	0.413	0.697	0.859	0.394	0.774	0.568	0.724	0.925	0.776	0.802	0.799	0.749	0.939
	REFECO	0.947	0.721	0.965	0.919	0.962	0.615	0.444	0.733	0.621	0.740	0.607	0.521	0.851	0.700	0.834	0.878	0.585	0.958	0.829	0.926
	OTASIAN	0.955	0.966	0.948	0.969	0.993	0.564	0.921	0.728	0.844	0.910	0.562	0.934	0.830	0.899	0.948	0.866	0.947	0.935	0.956	0.977
	ROW	0.767	0.000	0.923	0.000	0.000	0.452	0.000	0.707	0.000	0.000	0.461	0.000	0.776	0.000	0.000	0.675	0.000	0.868	0.000	0.000
	SUBSAFR	0.950	0.768	0.857	0.832	0.854	0.952	0.806	0.874	0.839	0.847	0.971	0.944	0.903	0.768	0.709	0.971	0.943	0.897	0.796	0.709
	CHN	0.969	0.925	0.961	0.958	0.926	0.963	0.928	0.960	0.958	0.907	0.970	0.934	0.978	0.961	0.879	0.971	0.930	0.983	0.972	0.876
	EUWE	0.896	0.919	0.693	0.835	0.970	0.871	0.908	0.685	0.824	0.969	0.939	0.889	0.660	0.684	0.964	0.946	0.889	0.630	0.757	0.967
	SOUASIA	0.910	0.545	0.939	0.834	0.909	0.898	0.756	0.938	0.837	0.915	0.920	0.615	0.963	0.817	0.888	0.920	0.611	0.975	0.820	0.914
	LATAME	0.939	0.618	0.948	0.067	0.903	0.927	0.625	0.948	0.089	0.885	0.949	0.597	0.967	-0.152	0.840	0.941	0.597	0.972	-0.121	0.832
N_2O	MIDEAST	0.873	0.726	0.957	0.979	0.910	0.858	0.729	0.956	0.980	0.911	0.904	0.530	0.968	0.987	0.931	0.901	0.547	0.966	0.990	0.940
	NORAM	0.891	0.873	0.871	0.854	0.913	0.870	0.878	0.896	0.853	0.913	0.916	0.911	0.925	0.795	0.938	0.919	0.911	0.920	0.836	0.940
	PACOECD	0.836	0.800	0.830	0.024	0.958	0.791	0.795	0.879	0.008	0.942	0.901	0.667	0.879	-0.069	0.916	0.910	0.659	0.881	-0.014	0.913
	REFECO	0.901	0.484	0.354	0.370	0.691	0.877	0.464	0.414	0.371	0.691	0.947	0.280	0.485	0.174	0.811	0.947	0.280	0.509	0.231	0.788
	OTASIAN	0.913	0.610	0.927	0.700	0.941	0.895	0.618	0.929	0.698	0.940	0.932	0.514	0.943	0.497	0.951	0.932	0.517	0.931	0.545	0.954
	ROW	0.000	0.000	0.806	0.000	0.998	0.000	0.000	0.840	0.000	0.000	0.000	0.000	0.833	0.000	0.000	0.000	0.000	0.866	0.000	0.000

Table 6. Statistical validation of regional emission pathways reproduced from ACC2-emIAM with original emission pathways from five ENGAGE IAMs. Ordinary Pearson's correlation coefficient r_P and Lin's concordance coefficient r_C are shown in the table. The higher the value of the indicator is, the darker the color of the cell is. This table presents the results from all scenarios. Results only from the ECB scenarios without INDC can be found in Table S6.

The statistics of the validation tests for global MAC curves are shown in Table 5. Those for regional MAC curves are in Table 6. The values of r_C are generally lower than the corresponding values of r_P, as expected. Reproducibility is generally higher for CO_2 than for CH_4 and N_2O. Certain models tend to have higher values for such indicators than other models. In the global case, AIM tends to show relatively low values for CH_4. IMAGE and TIAM tend to show low values for N_2O. In the regional results, these models give similar values for CO_2 for all Tests. The outcomes for CH_4 and N_2O are diverse and difficult to generalize. Finally, ROW is marked with low values in many models and from most of the Tests.

Deleted:

Deleted: 6.

Deleted: -ACC2

Deleted: figure

Deleted: Figure 11

Deleted: The reproducibility

Deleted: COFFEE gives lowest

Deleted: Test 1, but in other

Deleted: , it gives similar values with other models.

Deleted: outcome

Deleted: be generalized

5. Conclusions

We have developed emIAM, a novel modeling approach to emulating IAMs by using an extensive array of MAC curves: ten IAMs (nine ENGAGE IAMs and GET); global and ten regions; three gases (CO_2, CH_4, and N_2O); eight portfolios of available mitigation technologies; and two emission sources (total anthropogenic and energy-related). A series of four validation tests (Table 4) were performed using ACC2-emIAM, the hard-linked optimizing climate-economy model, to reproduce the original IAM outcomes. The results showed that the original emission pathways were reproduced reasonably well in the majority of cases (Tables 5 and 6), although the reproducibility varied depending on the IAM, region, gas, portfolio, source, test, and scenario type as summarized below.

- The validation results for the two long-lived gases CO_2 and N_2O did not strongly differ across all four tests, even though for Tests 2 to 4, there is a difference in the model setup between the original IAMs (GHG aggregation using GWP100) and ACC2-emIAM (individual gas cycle modeling without using GWP100). On the other hand, the validation results for the short-lived gas CH_4 in Tests 2 to 4 were not as good as those in Test 1. Test 4, with the additional mid-century temperature target, yielded higher reproducibility for CH_4 than Tests 2 and 3.
- Overall, the global emissions were better reproduced than the regional emissions. CO_2 emission pathways were generally better reproduced than CH_4 and N_2O pathways. Specific pathway features such as CO_2 emissions in 2030, 2050, and 2100, cumulative negative CO_2 emissions from 2020 to 2100, the year to net zero for CO_2, and that for GHG were reproduced to varying degrees across models and carbon budgets (Figure 10). While certain biases for some models were found for certain pathway features, as reported earlier, no general conclusions can be drawn.
- Some IAMs were more easily emulated than other IAMs, reflecting specific model features such as solution methods, technology assumptions, and abatement inertia. The emulator can usually reproduce the emission pathways of an IAM better if the model response to carbon price are well fitted with a MAC function.
- Certain data points were difficult to capture by MAC curves. In particular, PKB scenarios with low carbon budgets can give very large carbon prices in the near-term. Such data points tend to deviate from the trend of other data points and were manually removed from the MAC curve fitting where appropriate (Figure 1 and Table 1). Except for these "outliers," no discernible difference in the data trend was found between ECB scenarios and PKB scenarios, supporting the use of common MAC curves for ECB and PKB scenarios. Note also that certain data points from GET at high abatement levels do not follow the trend of other data points and were also removed from the MAC curve fitting where appropriate. We speculate that these data points are affected by the limit on CCS capacity assumed in GET.
- The overall good reproducibility of emIAM relies on the use of time-independent MAC curves for percentage emission reductions. The behaviors of IAMs that contain various time-dependent processes were generally well captured by the time-independent MAC curves. A plausible explanation is that the use of percentage abatement levels relative to rising baseline can offset the effect of lowering mitigation costs through learning.

Deleted: an extensive array
Deleted: a large set
Deleted: ten
Deleted: eleven
Deleted: the
Deleted: -ACC2
Deleted: the
Deleted: a
Deleted: (Tables 5 and 6), although the reproducibility varied depending on the IAM, region, gas, portfolio, source, test, and
Deleted: . However,

If one is interested in using emIAM, this could easily be done by combining the MAC curve(s), the limits on the abatement levels and their 1st and 2nd derivatives, and the baseline scenario of the IAM of interest in an optimization environment such as GAMS. We do not provide specific recommendations on the appropriateness of using each MAC curve and leave it up to the user to decide which MAC curves to use because the required accuracy of the IAM emulator depends on the purpose of the application. However, the goodness of fit of the MAC curves to the original IAM data and the results of validation tests should be carefully examined. Materials needed to make such decisions are systematically presented in Supplement and our Zenodo repository, in addition to the discussion above.

This study demonstrated 1) a methodological framework to generate MAC curves from multiple IAMs simulated under a range of carbon budgets and carbon price scenarios and 2) another methodological framework to assess the performance of MAC curves with a simple climate model to reproduce original IAM outcomes. Our methods are generic and transparent, providing an avenue for extending simple climate models to hard-linked climate-economy models. Future studies may emulate specific IAMs with more tailored parameterization approaches. We also open up an avenue for performing a quasi-multiple IAM analysis with low computational cost. Given the variety of IAMs available today, insights from multiple IAMs are indispensable for creating robust findings. Finally, simple models are complementary to complex models; modeling is an art that can shed light into the fundamental laws of complex systems (Yanai, 2009). In similar vein, emIAM can further pave an avenue for understanding the general behavior of IAMs.

Code availability. GAMS code (emIAM v1.0) for deriving MAC curves is archived on Zenode with doi: 10.5281/zenodo.7478234.

Data availability. Data for the parameters in MAC curves and associated upper limits on abatement levels and their first and second derivatives are available on Zenodo with doi:10.5281/zenodo.7478234. The supplement related to this article is also available online.

Author contributions. Conceptualization of the IAM emulator, W.X. and K.T.; simulations using ACC2-emIAM, W.X. and K.T.; simulations using GET, K.T, D.J., and M.L.; analysis of simulation results, W.X., K.T., and D.J.; writing - original draft preparation, W.X. and K.T.; writing – revision and editing, W.X., K.T., P.C., D.J., and M.L. All authors have read and agreed to the submitted version of the manuscript.

Competing interests. The authors declare that they have no conflict of interest.

Acknowledgments. K.T. dedicates this paper to the memory of Prof. Hiroshi Yanai (1937-2021) of Keio University, Tokyo, Japan, a pioneer in the field of Operations Research and his bachelor thesis advisor, by whom K.T. was taught the fundamentals of mathematical modeling and academic writing and the joy of intellectual pursuit. We would like to thank, in particular, but not limited to, the following individuals (in alphabetical order) for their valuable comments and related useful discussions: Nico Bauer, Thomas Bossy, Stéphane De Cara, Yann Gaucher, Xiangping Hu, Stuart Jenkins, Leon Merfort, Dale Rothman,

Deleted: We do not provide specific recommendations on the appropriateness of the use of each MAC curve and leave the users to decide which MAC curves to apply.

Deleted: that are required for making

Deleted: . Some IAMs were more easily emulated than other IAMs. The goodness of fit of the MAC curves depends on gases and regions

Deleted: a small

Deleted: In view of

Deleted: diversity

Deleted: -ACC2

Deleted: at

Deleted: supervisor

Deleted: are grateful

Deleted: from

Chris Smith, Xuanming Su, Kiyoshi Takahashi, Frank Venmans, Rintaro Yamaguchi, Tokuta Yokohata, and Theodoros Zachariadis. W.X. acknowledges financial support from the China Scholarship Council. This research was conducted as part of the Achieving the Paris Agreement Temperature Targets after Overshoot (PRATO) project under the Make Our Planet Great Again (MOPGA) program and funded by the National Research Agency in France under the Programme d'Investissements d'Avenir, grant number ANR-19-MPGA-0008. We further acknowledge the European Union's Horizon Europe research and innovation programme under Grant Agreements N° 101056939 (RESCUE – Response of the Earth System to overshoot, Climate neUtrality and negative Emissions) and N° 101081193 (OptimESM – Optimal High Resolution Earth System Models for Exploring Future Climate Changes) and the Environment Research and Technology Development Fund (JPMEERF20202002) of the Environmental Restoration and Conservation Agency (Japan).

Deleted: and

Deleted: which were useful for this study

Deleted: Project

Deleted: Program

Deleted: acknowledge

References

Akoglu, H.: User's guide to correlation coefficients, Turk. J. Emerg. Med., 18, 91–93, https://doi.org/10.1016/j.tjem.2018.08.001, 2018.

Allen, M. R., Peters, G. P., Shine, K. P., Azar, C., Balcombe, P., Boucher, O., Cain, M., Ciais, P., Collins, W., Forster, P. M., Frame, D. J., Friedlingstein, P., Fyson, C., Gasser, T., Hare, B., Jenkins, S., Hamburg, S. P., Johansson, D. J. A., Lynch, J., Macey, A., Morfeldt, J., Nauels, A., Ocko, I., Oppenheimer, M., Pacala, S. W., Pierrehumbert, R., Rogelj, J., Schaeffer, M., Schleussner, C. F., Shindell, D., Skeie, R. B., Smith, S. M., and Tanaka, K.: Indicate separate contributions of long-lived and short-lived greenhouse gases in emission targets, Npj Clim. Atmospheric Sci., 5, 5, https://doi.org/10.1038/s41612-021-00226-2, 2022.

Azar, C., Lindgren, K., and Andersson, B. A.: Global energy scenarios meeting stringent CO_2 constraints—cost-effective fuel choices in the transportation sector, Energy Policy, 31, 961–976, https://doi.org/10.1016/S0301-4215(02)00139-8, 2003.

Azar, C., Johansson, D. J. A., and Mattsson, N.: Meeting global temperature targets—the role of bioenergy with carbon capture and storage, Environ. Res. Lett., 8, 034004, https://doi.org/10.1088/1748-9326/8/3/034004, 2013.

Babiker, M., Gurgel, A., Paltsev, S., and Reilly, J.: Forward-looking versus recursive-dynamic modeling in climate policy analysis: A comparison, Econ. Model., 26, 1341–1354, https://doi.org/10.1016/j.econmod.2009.06.009, 2009.

Barnhart, H. X., Haber, M. J., and Lin, L. I.: An Overview on Assessing Agreement with Continuous Measurements, J. Biopharm. Stat., 17, 529–569, https://doi.org/10.1080/10543400701376480, 2007.

Berg, M. van den, Hof, A. F., Vliet, J. van, and Vuuren, D. P. van: Impact of the choice of emission metric on greenhouse gas abatement and costs, Environ. Res. Lett., 10, 024001, https://doi.org/10.1088/1748-9326/10/2/024001, 2015.

Bland, J. M. and Altman, D. G.: Statistical methods for assessing agreement between two methods of clinical measurement, The Lancet, 327, 307–310, https://doi.org/10.1016/S0140-6736(86)90837-8, 1986.

Bruckner, T., Hooss, G., Füssel, H.-M., and Hasselmann, K.: Climate system modeling in the framework of the tolerable windows approach: The ICLIPS climate model, Clim. Change, 56, 119–137, https://doi.org/10.1023/A:1021300924356, 2003.

Byers, E., Krey, V., Kriegler, E., Riahi, K., Schaeffer, R., Kikstra, J., Lamboll, R., Nicholls, Z., Sandstad, M., Smith, C., van der Wijst, K., Al -Khourdajie, A., Lecocq, F., Portugal-Pereira, J., Saheb, Y., Stromman, A., Winkler, H., Auer, C., Brutschin, E., Gidden, M., Hackstock, P., Harmsen, M., Huppmann, D., Kolp, P., Lepault, C., Lewis, J., Marangoni, G., Müller-Casseres, E., Skeie, R., Werning, M., Calvin, K., Forster, P., Guivarch, C., Hasegawa, T., Meinshausen, M., Peters, G., Rogelj, J., Samset, B., Steinberger, J., Tavoni, M., and van Vuuren, D.: AR6 Scenarios Database, https://doi.org/10.5281/zenodo.7197970, 2022.

Campiglio, E., Dietz, S., and Venmans, F.: Optimal Climate Policy As If the Transition Matters, SSRN Electron. J., https://doi.org/10.2139/ssrn.4307483, 2022.

National Research Council: Assessing the Reliability of Complex Models: Mathematical and Statistical Foundations of Verification, Validation, and Uncertainty Quantification, National Academies Press, Washington, D.C., https://doi.org/10.17226/13395, 2012.

Cox, N. J.: Assessing agreement of measurements and predictions in geomorphology, Geomorphology, 76, 332–346, https://doi.org/10.1016/j.geomorph.2005.12.001, 2006.

De Cara, S. and Jayet, P.-A.: Marginal abatement costs of greenhouse gas emissions from European agriculture, cost effectiveness, and the EU non-ETS burden sharing agreement, Ecol. Econ., 70, 1680–1690, https://doi.org/10.1016/j.ecolecon.2011.05.007, 2011.

Drouet, L., Bosetti, V., Padoan, S. A., Reis, L. A., Bertram, C., Longa, F. D., Després, J., Emmerling, J., Fosse, F., Fragkiadakis, K., Frank, S., Fricko, O., Fujimori, S., Harmsen, M., Krey, V., Oshiro, K., Nogueira, L. P., Paroussos, L., Piontek, F., Riahi, K., Rochedo, P. R. R., Schaeffer, R., Takakura, J., Wijst, K.-I. van der, Zwaan, B. van der, Vuuren, D.

Moved (insertion) [42]

van, Vrontisi, Z., Weitzel, M., Zakeri, B., and Tavoni, M.: Net zero-emission pathways reduce the physical and economic risks of climate change, Nat. Clim. Change, 11, 1070–1076, https://doi.org/10.1038/s41558-021-01218-z, 2021.

Ellerman, A. D. and Decaux, A.: Analysis of Post-Kyoto CO_2 Emissions Trading Using Marginal Abatement Curves, MIT Global Change, 1998.

Emmerling, J., Drouet, L., Wijst, K.-I. van der, Vuuren, D. van, Bosetti, V., and Tavoni, M.: The role of the discount rate for emission pathways and negative emissions, Environ. Res. Lett., 14, 104008, https://doi.org/10.1088/1748-9326/ab3cc9, 2019.

Errickson, F. C., Keller, K., Collins, W. D., Srikrishnan, V., and Anthoff, D.: Equity is more important for the social cost of methane than climate uncertainty, Nature, 592, 564–570, https://doi.org/10.1038/s41586-021-03386-6, 2021.

Fuglestvedt, J. S., Berntsen, T. K., Godal, O., Sausen, R., Shine, K. P., and Skodvin, T.: Metrics of climate change: assessing radiative forcing and emission indices, Clim. Change, 58, 267–331, https://doi.org/10.1023/A:1023905326842, 2003.

Gaucher, Y., Tanaka, K., Johansson, D., Goll, D., and Ciais, P.: Leveraging ecosystems responses to enhanced rock weathering in mitigation scenarios, https://doi.org/10.21203/rs.3.rs-3145606/v1, 27 July 2023.

Guivarch, C. and Rogelj, J.: Carbon price variations in 2°C scenarios explored, https://www.carbonpricingleadership.org/s/Guivarch-Rogelj-Carbon-prices-2C.pdf, January 2017.

Guivarch, C., Kriegler, E., Portugal-Pereira, J., Bosetti, V., Edmonds, J., Fischedick, M., Havlík, P., Jaramillo, P., Krey, V., Lecocq, F., Lucena, A., Meinshausen, M., Mirasgedis, S., O'Neill, B., Peters, G. P., Rogelj, J., Rose, S., Saheb, Y., Strbac, G., Strømman, A. H., Vuuren, D. P. van, and Zhou, N.: IPCC, 2022: Annex III: Scenarios and modelling methods, in: IPCC, 2022: Climate Change 2022: Mitigation of Climate Change. Contribution of Working Group III to the Sixth Assessment Report of the Intergovernmental Panel on Climate Change, Cambridge University Press, Cambridge, UK and New York, NY, USA, 2022.

Ha-Duong, M., Grubb, M. J., and Hourcade, J.-C.: Influence of socioeconomic inertia and uncertainty on optimal CO_2-emission abatement, Nature, 390, 270–273, https://doi.org/10.1038/36825, 1997.

Harmsen, J. H. M., van Vuuren, D. P., Nayak, D. R., Hof, A. F., Höglund-Isaksson, L., Lucas, P. L., Nielsen, J. B., Smith, P., and Stehfest, E.: Long-term marginal abatement cost curves of non-CO_2 greenhouse gases, Environ. Sci. Policy, 99, 136–149, https://doi.org/10.1016/j.envsci.2019.05.013, 2019.

Harmsen, M. J. H. M., Berg, M. van den, Krey, V., Luderer, G., Marcucci, A., Strefler, J., and Vuuren, D. P. V.: How climate metrics affect global mitigation strategies and costs: a multi-model study, Clim. Change, 136, 203–216, https://doi.org/10.1007/s10584-016-1603-7, 2016.

Hasselmann, K., Hasselmann, S., Giering, R., Ocana, V., and Storch, H. v.: Sensitivity Study of Optimal CO_2 Emission Paths Using a Simplified Structural Integrated Assessment Model (SIAM), Clim. Change, 37, 345–386, https://doi.org/10.1023/A:1005339625015, 1997.

Hayashi, F.: Econometrics, Princeton University Press, Princeton, 683 pp., 2000.

Hedenus, F., Karlsson, S., Azar, C., and Sprei, F.: Cost-effective energy carriers for transport – The role of the energy supply system in a carbon-constrained world, Int. J. Hydrog. Energy, 35, 4638–4651, https://doi.org/10.1016/j.ijhydene.2010.02.064, 2010.

Hof, A. F., Wijst, K.-I. van der, and Vuuren, D. P. van: The Impact of Socio-Economic Inertia and Restrictions on Net-Negative Emissions on Cost-Effective Carbon Price Pathways, Front. Clim., 3, 785577, https://doi.org/10.3389/fclim.2021.785577, 2021.

Hooss, G., Voss, R., Hasselmann, K., Maier-Reimer, E., and Joos, F.: A nonlinear impulse response model of the coupled carbon cycle-climate system (NICCS), Clim. Dyn., 18, 189–202, https://doi.org/10.1007/s003820100170, 2001.

Huang, S. K., Kuo, L., and Chou, K.-L.: The applicability of marginal abatement cost approach: A comprehensive review,

J. Clean. Prod., 127, 59–71, https://doi.org/10.1016/j.jclepro.2016.04.013, 2016.

IPCC: Summary for Policymakers, in: Climate Change 2013: The Physical Science Basis. Contribution of Working Group I to the Fifth Assessment Report of the Intergovernmental Panel on Climate Change, Cambridge University Press, Cambridge, United Kingdom and New York, NY, USA, 2013.

IPCC: Summary for Policymakers, in: Climate Change 2021: The Physical Science Basis. Contribution of Working Group I to the Sixth Assessment Report of the Intergovernmental Panel on Climate Change, Cambridge University Press, Cambridge, United Kingdom and New York, NY, USA, 3–32, 2021.

Jiang, H.-D., Dong, K.-Y., Zhang, K., and Liang, Q.-M.: The hotspots, reference routes, and research trends of marginal abatement costs: A systematic review, J. Clean. Prod., 252, 119809, https://doi.org/10.1016/j.jclepro.2019.119809, 2020.

Jiang, H.-D., Purohit, P., Liang, Q.-M., Dong, K., and Liu, L.-J.: The cost-benefit comparisons of China's and India's NDCs based on carbon marginal abatement cost curves, Energy Econ., 109, 105946, https://doi.org/10.1016/j.eneco.2022.105946, 2022.

Johansson, D. J. A.: Temperature stabilization, ocean heat uptake and radiative forcing overshoot profiles, Clim. Change, 108, 107–134, https://doi.org/10.1007/s10584-010-9969-4, 2011.

Johansson, D. J. A.: The question of overshoot, Nat. Clim. Change, 11, 1021–1022, https://doi.org/10.1038/s41558-021-01229-w, 2021.

Johansson, D. J. A., Persson, U. M., and Azar, C.: The cost of using global warming potentials: Analysing the trade off between CO_2, CH_4 and N_2O, Clim. Change, 77, 291–309, https://doi.org/10.1007/s10584-006-9054-1, 2006.

Joos, F., Roth, R., Fuglestvedt, J. S., Peters, G. P., Enting, I. G., Bloh, W. von, Brovkin, V., Burke, E. J., Eby, M., Edwards, N. R., Friedrich, T., Frölicher, T. L., Halloran, P. R., Holden, P. B., Jones, C., Kleinen, T., Mackenzie, F. T., Matsumoto, K., Meinshausen, M., Plattner, G.-K., Reisinger, A., Segschneider, J., Shaffer, G., Steinacher, M., Strassmann, K., Tanaka, K., Timmermann, A., and Weaver, A. J.: Carbon dioxide and climate impulse response functions for the computation of greenhouse gas metrics: a multi-model analysis, Atmospheric Chem. Phys., 13, 2793–2825, https://doi.org/10.5194/acp-13-2793-2013, 2013.

Kesicki, F.: Marginal abatement cost curves: Combining energy system modelling and decomposition analysis, Environ. Model. Assess., 18, 27–37, https://doi.org/10.1007/s10666-012-9330-6, 2013.

Kesicki, F. and Ekins, P.: Marginal abatement cost curves: a call for caution, Clim. Policy, 12, 219–236, https://doi.org/10.1080/14693062.2011.582347, 2012.

Kesicki, F. and Strachan, N.: Marginal abatement cost (MAC) curves: confronting theory and practice, Environ. Sci. Policy, 14, 1195–1204, https://doi.org/10.1016/j.envsci.2011.08.004, 2011.

Klepper, G. and Peterson, S.: Marginal abatement cost curves in general equilibrium: The influence of world energy prices, Resour. Energy Econ., 28, 1–23, https://doi.org/10.1016/j.reseneeco.2005.04.001, 2006.

Kriegler, E.: Imprecise probability analysis for integrated assessment of climate change, Universität Potsdam, Germany, 2005.

Lashof, D. A. and Ahuja, D. R.: Relative contributions of greenhouse gas emissions to global warming, Nature, 344, 529–531, https://doi.org/10.1038/344529a0, 1990.

Laws, E. A.: Mathematical methods for oceanographers: an introduction, Wiley, New York, 343 pp., 1997.

Leach, N. J., Jenkins, S., Nicholls, Z., Smith, C. J., Lynch, J., Cain, M., Walsh, T., Wu, B., Tsutsui, J., and Allen, M. R.: FaIRv2.0.0: a generalized impulse response model for climate uncertainty and future scenario exploration, Geosci. Model Dev., 14, 3007–3036, https://doi.org/10.5194/gmd-14-3007-2021, 2021.

Lehtveer, M. and Hedenus, F.: Nuclear power as a climate mitigation strategy – technology and proliferation risk, J. Risk Res., 18, 273–290, https://doi.org/10.1080/13669877.2014.889194, 2015.

Lehtveer, M., Brynolf, S., and Grahn, M.: What Future for Electrofuels in Transport? Analysis of Cost Competitiveness in Global Climate Mitigation, Environ. Sci. Technol., 53, 1690–1697, https://doi.org/10.1021/acs.est.8b05243, 2019.

Levasseur, A., Cavalett, O., Fuglestvedt, J. S., Gasser, T., Johansson, D. J. A., Jørgensen, S. V., Raugei, M., Reisinger, A., Schivley, G., Strømman, A., Tanaka, K., and Cherubini, F.: Enhancing life cycle impact assessment from climate science: Review of recent findings and recommendations for application to LCA, Ecol. Indic., 71, 163–174, https://doi.org/10.1016/j.ecolind.2016.06.049, 2016.

Lin, L., Hedayat, A. S., and Wu, W.: Continuous Data, in: Statistical Tools for Measuring Agreement, Springer New York, New York, NY, 7–54, https://doi.org/10.1007/978-1-4614-0562-7_2, 2012.

Lin, L. I.-K.: A Concordance Correlation Coefficient to Evaluate Reproducibility, Biometrics, 45, 255, https://doi.org/10.2307/2532051, 1989.

Mackenzie, F. T. and Lerman, A.: Carbon in the geobiosphere: earth's outer shell, Springer, Dordrecht, 402 pp., 2006.

Mastropierro, M., Tanaka, K., Melnikova, I., and Ciais, P.: Testing GWP* to quantify non-CO_2 contributions in the carbon budget framework: the case under overshoot scenarios, In Review, https://doi.org/10.21203/rs.3.rs-3206717/v1, 2023.

Matthews, H. D., Gillett, N. P., Stott, P. A., and Zickfeld, K.: The proportionality of global warming to cumulative carbon emissions, Nature, 459, 829–832, https://doi.org/10.1038/nature08047, 2009.

McKeough, P.: A case for ensuring reductions in CO_2 emissions are given priority over reductions in CH4 emissions in the near term, Clim. Change, 174, 4, https://doi.org/10.1007/s10584-022-03428-6, 2022.

McKinsey & Company: Pathways to a low-carbon economy: Version 2 of the global greenhouse gas abatement cost curve, 2009.

Melnikov, N. B., Gruzdev, A. P., Dalton, M. G., Weitzel, M., and O'Neill, B. C.: Parallel Extended Path Method for Solving Perfect Foresight Models, Comput. Econ., 58, 517–534, https://doi.org/10.1007/s10614-020-10044-y, 2021.

Melnikova, I., Boucher, O., Cadule, P., Ciais, P., Gasser, T., Quilcaille, Y., Shiogama, H., Tachiiri, K., Yokohata, T., and Tanaka, K.: Carbon cycle response to temperature overshoot beyond 2°C: An analysis of CMIP6 models, Earths Future, 9, https://doi.org/10.1029/2020EF001967, 2021.

Morris, J., Paltsev, S., and Reilly, J.: Marginal Abatement Costs and Marginal Welfare Costs for Greenhouse Gas Emissions Reductions: Results from the EPPA Model, Environ. Model. Assess., 17, 325–336, https://doi.org/10.1007/s10666-011-9298-7, 2012.

Mulugeta, L., Drach, A., Erdemir, A., Hunt, C. A., Horner, M., Ku, J. P., Jr., J. G. M., Vadigepalli, R., and Lytton, W. W.: Credibility, Replicability, and Reproducibility in Simulation for Biomedicine and Clinical Applications in Neuroscience, Front. Neuroinformatics, 12, 18, https://doi.org/10.3389/fninf.2018.00018, 2018.

Nicholls, Z. R. J., Meinshausen, M., Lewis, J., Gieseke, R., Dommenget, D., Dorheim, K., Fan, C.-S., Fuglestvedt, J. S., Gasser, T., Golüke, U., Goodwin, P., Hartin, C., Hope, A. P., Kriegler, E., Leach, N. J., Marchegiani, D., McBride, L. A., Quilcaille, Y., Rogelj, J., Salawitch, R. J., Samset, B. H., Sandstad, M., Shiklomanov, A. N., Skeie, R. B., Smith, C. J., Smith, S., Tanaka, K., Tsutsui, J., and Xie, Z.: Reduced complexity model intercomparison project phase 1: introduction and evaluation of global-mean temperature response, Geosci. Model Dev., 13, 5175–5190, https://doi.org/10.5194/gmd-13-5175-2020, 2020.

Nordhaus, W. D.: The Cost of Slowing Climate Change: a Survey, Energy J., 12, https://doi.org/10.5547/ISSN0195-6574-EJ-Vol12-No1-4, 1991.

Nordhaus, W. D.: Revisiting the social cost of carbon, Proc. Natl. Acad. Sci., 114, 1518–1523, https://doi.org/10.1073/pnas.1609244114, 2017.

O'Neill, B. C.: Economics, Natural Science, and the Costs of Global Warming Potentials, Clim. Change, 58, 251–260, https://doi.org/10.1023/A:1023968127813, 2003.

Moved up [42]: National Research Council: Assessing the Reliability of Complex Models: Mathematical and Statistical Foundations of Verification, Validation, and Uncertainty Quantification, National Academies Press, Washington, D.C., https://doi.org/10.17226/13395, 2012.

Deleted: Oliveira, T. D., Brunelle, T., Guenet, B., Ciais, P., Leblanc, F., and Guivarch, C.: A mixed-effect model approach for assessing land-based mitigation in integrated assessment models: A regional perspective, Glob. Change Biol., 27, 4671–4685, https://doi.org/10.1111/gcb.15738, 2021.

O'Neill, B. C., Tebaldi, C., Vuuren, D. P. van, Eyring, V., Friedlingstein, P., Hurtt, G., Knutti, R., Kriegler, E., Lamarque, J.-F., Lowe, J., Meehl, G. A., Moss, R., Riahi, K., and Sanderson, B. M.: The Scenario Model Intercomparison Project (ScenarioMIP) for CMIP6, Geosci. Model Dev., 9, 3461–3482, https://doi.org/10.5194/gmd-9-3461-2016, 2016.

Reisinger, A., Havlik, P., Riahi, K., Vliet, O. van, Obersteiner, M., and Herrero, M.: Implications of alternative metrics for global mitigation costs and greenhouse gas emissions from agriculture, Clim. Change, 117, 677–690, https://doi.org/10.1007/s10584-012-0593-3, 2013.

Rennert, K., Errickson, F., Prest, B. C., Rennels, L., Newell, R. G., Pizer, W., Kingdon, C., Wingenroth, J., Cooke, R., Parthum, B., Smith, D., Cromar, K., Diaz, D., Moore, F. C., Müller, U. K., Plevin, R. J., Raftery, A. E., Ševčíková, H., Sheets, H., Stock, J. H., Tan, T., Watson, M., Wong, T. E., and Anthoff, D.: Comprehensive evidence implies a higher social cost of CO_2, Nature, 610, 687–692, https://doi.org/10.1038/s41586-022-05224-9, 2022.

Riahi, K., Vuuren, D. P. van, Kriegler, E., Edmonds, J., O'Neill, B. C., Fujimori, S., Bauer, N., Calvin, K., Dellink, R., Fricko, O., Lutz, W., Popp, A., Cuaresma, J. C., Kc, S., Leimbach, M., Jiang, L., Kram, T., Rao, S., Emmerling, J., Ebi, K., Hasegawa, T., Havlik, P., Humpenöder, F., Silva, L. A. D., Smith, S., Stehfest, E., Bosetti, V., Eom, J., Gernaat, D., Masui, T., Rogelj, J., Strefler, J., Drouet, L., Krey, V., Luderer, G., Harmsen, M., Takahashi, K., Baumstark, L., Doelman, J. C., Kainuma, M., Klimont, Z., Marangoni, G., Lotze-Campen, H., Obersteiner, M., Tabeau, A., and Tavoni, M.: The Shared Socioeconomic Pathways and their energy, land use, and greenhouse gas emissions implications: An overview, Glob. Env. Chang, 42, 153–168, https://doi.org/10.1016/j.gloenvcha.2016.05.009, 2017.

Riahi, K., Bertram, C., Huppmann, D., Rogelj, J., Bosetti, V., Cabardos, A.-M., Deppermann, A., Drouet, L., Frank, S., Fricko, O., Fujimori, S., Harmsen, M., Hasegawa, T., Krey, V., Luderer, G., Paroussos, L., Schaeffer, R., Weitzel, M., Zwaan, B. van der, Vrontisi, Z., Longa, F. D., Després, J., Fosse, F., Fragkiadakis, K., Gusti, M., Humpenöder, F., Keramidas, K., Kishimoto, P., Kriegler, E., Meinshausen, M., Nogueira, L. P., Oshiro, K., Popp, A., Rochedo, P. R. R., Ünlü, G., Ruijven, B. van, Takakura, J., Tavoni, M., Vuuren, D. van, and Zakeri, B.: Cost and attainability of meeting stringent climate targets without overshoot, Nat. Clim. Change, 11, 1063–1069, https://doi.org/10.1038/s41558-021-01215-2, 2021.

Ricker, W. E.: Linear Regressions in Fishery Research, J. Fish. Res. Board Can., 30, 409–434, https://doi.org/10.1139/f73-072, 1973.

Schwoon, M. and Tol, R. S. J.: Optimal CO_2-abatement with Socio-economic Inertia and Induced Technological Change, Energy J., 27, https://doi.org/10.5547/ISSN0195-6574-EJ-Vol27-No4-2, 2006.

Shoemaker, J. K., Schrag, D. P., Molina, M. J., and Ramanathan, V.: What Role for Short-Lived Climate Pollutants in Mitigation Policy?, Science, 342, 1323–1324, https://doi.org/10.1126/science.1240162, 2013.

Su, X., Takahashi, K., Fujimori, S., Hasegawa, T., Tanaka, K., Kato, E., Shiogama, H., Masui, T., and Emori, S.: Emission pathways to achieve 2.0°C and 1.5°C climate targets, Earths Future, 5, 592–604, https://doi.org/10.1002/2016EF000492, 2017.

Sun, T., Ocko, I. B., Sturcken, E., and Hamburg, S. P.: Path to net zero is critical to climate outcome, Sci. Rep., 11, 22173, https://doi.org/10.1038/s41598-021-01639-y, 2021.

Tachiiri, K., Hajima, T., and Kawamiya, M.: Increase of the transient climate response to cumulative carbon emissions with decreasing CO_2 concentration scenarios, Environ. Res. Lett., 14, 124067, https://doi.org/10.1088/1748-9326/ab57d3, 2019.

Tanaka, K. and Mackenzie, F. T.: Ecosystem behavior of southern Kaneohe Bay, Hawaii: A statistical and modelling approach, Ecol. Model., 188, 296–326, https://doi.org/10.1016/j.ecolmodel.2005.02.018, 2005.

Tanaka, K. and O'Neill, B. C.: The Paris Agreement zero-emissions goal is not always consistent with the 1.5 °C and 2 °C temperature targets, Nat. Clim. Change, 8, 319–324, https://doi.org/10.1038/s41558-018-0097-x, 2018.

Tanaka, K. and Raddatz, T.: Correlation between climate sensitivity and aerosol forcing and its implication for the "climate trap": A Letter, Clim. Change, 109, 815–825, https://doi.org/10.1007/s10584-011-0323-2, 2011.

Tanaka, K., Kriegler, E., Bruckner, T., Hooss, G., Knorr, W., and Raddatz, T.: Aggregated Carbon Cycle, Atmospheric

Deleted: Riahi, K., Schaeffer, R., Arango, J., Calvin, K., Hasegawa, T., Jiang, K., Kriegler, E., Matthews, R., Robertson, S., Sebbit, A. M., Steinberger, J., Khourdajie, A. A., Brutschin, E., Byers, E., Carleton, T., Clarke, L., Chaturvedi, V., Chen, W., and Martínez, J. T.: Mitigation pathways compatible with long-term goals, in: IPCC, 2022: Climate Change 2022: Mitigation of Climate Change. Contribution of Working Group III to the Sixth Assessment Report of the Intergovernmental Panel on Climate Change, Cambridge University Press, Cambridge, UK and New York, NY, USA, 2022.

Deleted: Su, X., Tachiiri, K., Tanaka, K., Watanabe, M., and Kawamiya, M.: Identifying crucial emission sources under low forcing scenarios by a comprehensive attribution analysis, One Earth, S2590332222005358, https://doi.org/10.1016/j.oneear.2022.10.009, 2022.

Chemistry, and Climate Model (ACC2) – description of the forward and inverse modes, 2007.

Tanaka, K., O'Neill, B. C., Rokityanskiy, D., Obersteiner, M., and Tol, R. S. J.: Evaluating global warming potentials with historical temperature, Clim. Change, 96, 443–466, https://doi.org/10.1007/s10584-009-9566-6, 2009a.

Tanaka, K., Raddatz, T., O'Neill, B. C., and Reick, C. H.: Insufficient forcing uncertainty underestimates the risk of high climate sensitivity, Geophys. Res. Lett., 36, 6, https://doi.org/10.1029/2009GL039642, 2009b.

Tanaka, K., Peters, G. P., and Fuglestvedt, J. S.: Policy Update: Multicomponent climate policy: why do emission metrics matter?, Carbon Manag., 1, 191–197, https://doi.org/10.4155/cmt.10.28, 2010.

Tanaka, K., Johansson, D. J. A., O'Neill, B. C., and Fuglestvedt, J. S.: Emission metrics under the 2 °C climate stabilization target, Clim. Change, 117, 933–941, https://doi.org/10.1007/s10584-013-0693-8, 2013.

Tanaka, K., Cavalett, O., Collins, W. J., and Cherubini, F.: Asserting the climate benefits of the coal-to-gas shift across temporal and spatial scales, Nat. Clim. Change, 9, 389–396, https://doi.org/10.1038/s41558-019-0457-1, 2019.

Tanaka, K., Boucher, O., Ciais, P., Johansson, D. J. A., and Morfeldt, J.: Cost-effective implementation of the Paris Agreement using flexible greenhouse gas metrics, Sci. Adv., 7, eabf9020, https://doi.org/10.1126/sciadv.abf9020, 2021.

Tebaldi, C., Debeire, K., Eyring, V., Fischer, E., Fyfe, J., Friedlingstein, P., Knutti, R., Lowe, J., O'Neill, B., Sanderson, B., Van Vuuren, D., Riahi, K., Meinshausen, M., Nicholls, Z., Tokarska, K. B., Hurtt, G., Kriegler, E., Lamarque, J.-F., Meehl, G., Moss, R., Bauer, S. E., Boucher, O., Brovkin, V., Byun, Y.-H., Dix, M., Gualdi, S., Guo, H., John, J. G., Kharin, S., Kim, Y., Koshiro, T., Ma, L., Olivié, D., Panickal, S., Qiao, F., Rong, X., Rosenbloom, N., Schupfner, M., Séférian, R., Sellar, A., Semmler, T., Shi, X., Song, Z., Steger, C., Stouffer, R., Swart, N., Tachiiri, K., Tang, Q., Tatebe, H., Voldoire, A., Volodin, E., Wyser, K., Xin, X., Yang, S., Yu, Y., and Ziehn, T.: Climate model projections from the Scenario Model Intercomparison Project (ScenarioMIP) of CMIP6, Earth Syst. Dyn., 12, 253–293, https://doi.org/10.5194/esd-12-253-2021, 2021.

Thomson, R. E. and Emery, W. J.: Statistical Methods and Error Handling, in: Data Analysis Methods in Physical Oceanography, Elsevier, 219–311, https://doi.org/10.1016/B978-0-12-387782-6.00003-X, 2014.

Tol, R. S. J., Berntsen, T. K., O'Neill, B. C., Fuglestvedt, J. S., and Shine, K. P.: A unifying framework for metrics for aggregating the climate effect of different emissions, Environ. Res. Lett., 7, 044006, https://doi.org/10.1088/1748-9326/7/4/044006, 2012.

Tsutsui, J.: Minimal CMIP Emulator (MCE v1.2): a new simplified method for probabilistic climate projections, Geosci. Model Dev., 15, 951–970, https://doi.org/10.5194/gmd-15-951-2022, 2022.

UNFCCC: "Report of the Conference of the Parties serving as the meeting of the Parties to the Paris Agreement on the third part of its first session, held in Katowice from 2 to 15 December 2018. Addendum 2. Part two: Action taken by the Conference of the Parties serving as the meeting of the Parties to the Paris Agreement" (FCCC/PA/CMA/2018/3/ Add.2 2019), 2018.

UNFCCC: "In-session technical workshop on findings on emission metrics contained in the Sixth Assessment Report of the Intergovernmental Panel on Climate Change" (FCCC/SBSTA/2023/INF.2), Bonn, 2023.

Vermont, B. and De Cara, S.: How costly is mitigation of non-CO_2 greenhouse gas emissions from agriculture?, Ecol. Econ., 69, 1373–1386, https://doi.org/10.1016/j.ecolecon.2010.02.020, 2010.

Vuuren, D. P. van, Vries, B. de, Eickhout, B., and Kram, T.: Responses to technology and taxes in a simulated world, Energy Econ., 26, 579–601, https://doi.org/10.1016/j.eneco.2004.04.027, 2004.

Wagner, F., Amann, M., Borken-Kleefeld, J., Cofala, J., Höglund-Isaksson, L., Purohit, P., Rafaj, P., Schöpp, W., and Winiwarter, W.: Sectoral marginal abatement cost curves: implications for mitigation pledges and air pollution co-benefits for Annex I countries, Sustain. Sci., 7, 169–184, https://doi.org/10.1007/s11625-012-0167-3, 2012.

Weyant, J.: Some contributions of integrated assessment models of global climate change, Rev. Environ. Econ. Policy, 11, 115–137, https://doi.org/10.1093/reep/rew018, 2017.

IAMC_wiki: https://www.iamcdocumentation.eu/index.php/IAMC_wiki, last access: 28 October 2022.

Xiong, W., Tanaka, K., Ciais, P., and Yan, L.: Evaluating China's role in achieving the 1.5 °C Target of the Paris Agreement, Energies, 15, 6002, https://doi.org/10.3390/en15166002, 2022.

Yanai, H.: Mathematical models (in Japanese), Asakura Publishing Co., Ltd., Tokyo, Japan, 2009.

Yue, X., Deane, J. P., O'Gallachoir, B., and Rogan, F.: Identifying decarbonisation opportunities using marginal abatement cost curves and energy system scenario ensembles, Appl. Energy, 276, 115456, https://doi.org/10.1016/j.apenergy.2020.115456, 2020.

Zickfeld, K., Azevedo, D., Mathesius, S., and Matthews, H. D.: Asymmetry in the climate–carbon cycle response to positive and negative CO_2 emissions, Nat. Clim. Change, 11, 613–617, https://doi.org/10.1038/s41558-021-01061-2, 2021.